TRANSPORT PROCESSES ACCOMPANYING FREEZING

by

CHON SHON CHENG

B.S., National Taiwan University, 1964

A MASTER'S THESIS

submitted in partial fulfillment of the

requirements for the degree

MASTER OF SCIENCE

Department of Chemical Engineering

KANSAS STATE UNIVERSITY

Manhattan, Kansas

1967

Approved by:

Major Professor

TABLE OF CONTENTS

I. INTRODUCTION

The progressive freezing of a liquid charge, known as Normal Freezing, has long been used for purification of materials. However, not until ultrahigh-purity germanium was needed for semi-conductor work was much thought given to theoretical analysis of normal freezing.

The first quantitative investigation of this process and the related process of zone melting was undertaken by Pfann (1) in 1952. Since then, the successful application of these processes has aroused considerable interest in applications of the processes and has stimulated study of the accompanying transport phenomenon.

From the theoretical point of view, this process is equivalent to single-crystal pulling. The fundamental principle employed in the separation of solute (impurity) from the solvent during normal freezing is based on the fact that, when a solution solidifies, the equilibrium composition of the originating solid phase differs from the composition of the liquid phase. In other words, the separation basically depends on the phase equilibrium behavior of the solution charged. Therefore, for an understanding of segregation phenomena in normal freezing and related processes, it is essential to consider, firstly, the equilibrium behavior of the solvent (major component in mixture) and the solute (impurity) as described by their phase diagrams.

A. General Discussion of Phase Diagrams

There are various types of binary equilibrium diagrams. In many cases, those diagrams become quite complicated; however, they usually can be considered as combinations of the simpler types of systems. Therefore, a complete understanding of the simple types of systems will allow interpretation of the most complicated phase diagrams encountered. For the purpose of this study, consideration will be given to only two of these simple types: simple eutectic systems and solid solution systems.

Simple Binary Eutectic System

The simple binary eutectic phase diagram is shown in Figure 1-1. In this type of system, solutions of two components A and B always yield only pure A or pure B as solid phases. Point C and D represent the melting points of pure A and pure B respectively.

The curve CG represents the concentrations of solutions saturated with A at temperatures between C and F. In a like manner, curve DG represents the concentrations of solutions saturated with B at temperatures between D and H. At point G, three phases are in equilibrium; namely, a solution saturated with A and B, solid phase A, and solid phase B. A lowering of temperature below F must result in the complete solidification of solution G. The temperature F is named the "eutectic temperature" and the composition E, the "eutectic composition."

The phase behavior is best understood by considering what happens when cooling a mixture of A and B. If an unsaturated mixture of composition x_1 at temperature t_1 is cooled, only a drop in temperature

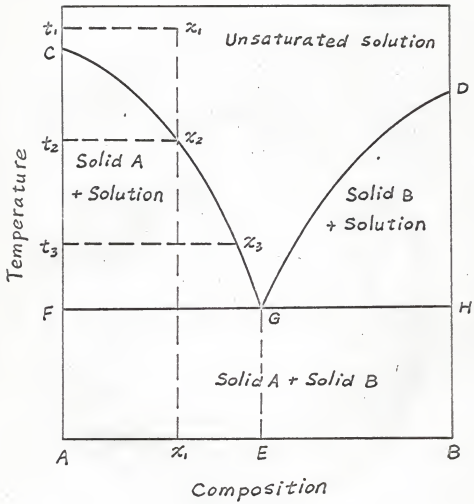

Fig. 1-1 Simple eutectic phase-diagram for a binary mixture.

results until the temperature t_2 is reached. At this point, t_2, x_2, the solution becomes saturated and a small drop in temperature t_2 causes solidification. The solid phase will be pure A and this solid is in equilibrium with the saturated solution of composition x_2. Continued cooling results in additional pure A separating out, and the composition of the saturated solution changes along line CG. At a temperature of t_3, pure solid A is in equilibrium with a saturated solution of composition x_3. When the temperature F is reached, another solid phase B appears. Further cooling causes A and B to crystallize from the saturated solution in the fixed composition E; this crystallization will continue until all of the solution has solidified. When the composition of the system is within the area CFG, solid crystals of pure A may be removed. Similarly, pure B can be obtained when starting with compositions between points E and B.

Binary Solid Solution System

In the same manner that two liquids may dissolve in each other to form a liquid solution, two solids may dissolve in each other to form a solid solution. These solutions are homogeneous and their compositions may vary over wide limits. Figure 1-2 shows the phase diagram for the case where the melting points of all solutions are between those of the pure components. Although not shown for this type of system, these curves can exhibit a maximum or a minimum.

In this diagram, points C and D represent the melting points of pure A and B respectively. The upper, or liquidus, curve indicates the temperature and composition of the saturated liquid solution. Points on this curve give the temperature of the initial solidification. The

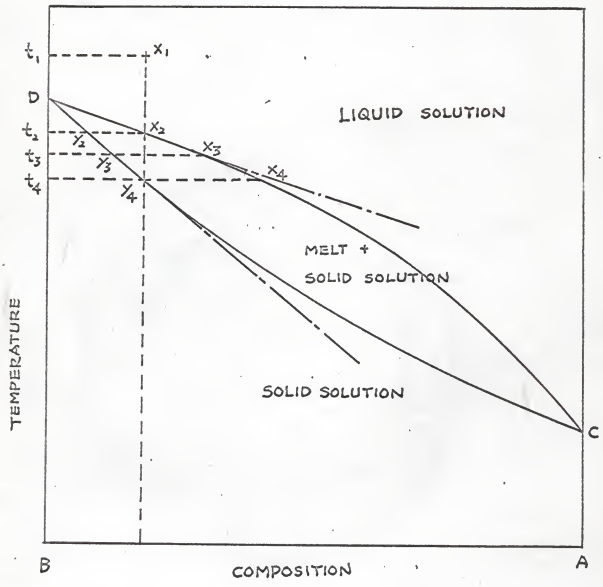

Fig. 1-2. SIMPLE PHASE DIAGRAM FOR A BINARY SOLID SOLUTION SYSTEM.

lower, or solidus, curve indicates the temperature at which the final solidification or initial melting occurs. Any horizontal line, such as x_2y_2, indicates compositions of the liquid and solid phase which are in equilibrium at the temperature t_2. Cooling a liquid solution of composition x_1, at temperature t_1, to temperature t_2 only results in a drop of the temperature. At this point, a lowering of the temperature will result in the formation of a small amount of solid solution of composition y_2. Thus, the composition of the melt will change and move towards x_3. Further cooling to t_3 will cause the composition of the solid solution to change to y_3, thus depleting A from the liquid and causing the liquid concentration to approach x_3. As cooling continues, the composition of the melt will change along the liquidus line towards point C, and the composition of the solid solution will change along the solidus line in the same direction. When temperature t_4 is reached, an infinitesimal amount of melt of composition x_4 will be in equilibrium with the solid solution of composition y_4, the same composition as the original melt x_1, and the mixture will be completely solidified.

In practice, and for the reason of simplicity in theoretical analysis of the freezing process, it is convenient to approximate the phase diagram with straight liquidus and solidus lines for dilute solutions of solid solution systems as shown in Figure 1-2. The restriction to low solute concentrations is not a serious limitation, as normal freezing is usually applied to just such cases. Hence, it is convenient to describe the salient feature of solid-liquid equilibrium by means of equilibrium distribution coefficient, K_o, the ratio of concentrations of the solid and the liquid in equilibrium, i.e. C_s/C. Due to the assumption of straight liquidus and solidus lines, this coefficient can be considered

as a constant for a given solid solution system. Obviously, the equilibrium distribution coefficient is zero for eutectic systems.

B. General Discussion of Normal Freezing

Normal freezing is a process developed to purify impure materials by freezing. During normal freezing of systems of initially uniform concentration, equilibrium between solid and liquid exists only at the freezing interface, and the solute (impurity) is rejected by the freezing solid. For both eutectic and solid solution systems ($K_o < 1$), a redistribution of the solute occurs. A qualitative description of the redistribution for a solid solution system is shown in Figure 1-3.

From a theoretical viewpoint, the solute redistribution curve in a solid must satisfy the following conditions: (1) It must rise from K_oC_o at the beginning of the crystal. (2) The area between C_o and C_s must be equal to the area between C_L and C_o for conservation of solute.

For solid solution systems, Pfann (1) developed a theoretical expression for solute redistribution in the solid with the assumptions that diffusion of the solute in the solid is negligible and mixing in the liquid phase is complete. The assumption of complete mixing in the liquid phase, however, is questionable from a practical point of view.

Tiller, Jackson, Rutter, and Chalmers (2) have derived an expression for solute redistribution assuming that liquid phase mixing is negligible and mass transfer in the liquid is due only to diffusion. Their expressions for the concentration profile in both the liquid and solid phases were first obtained for the steady state condition. Then the expressions of solute redistribution were obtained with the assumption that both

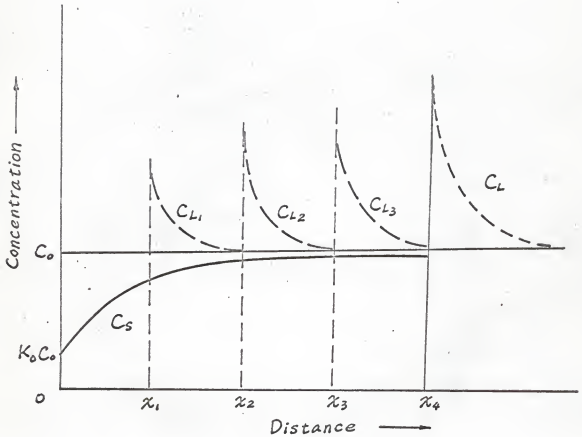

Fig. 1-3 Redistribution of solute in the liquid, C_L, and in the solid, C_s, during normal freezing. x's show the position of the growing interface at various times.

profiles will approach the steady state results exponentially without changing the "shape" of the profile in the liquid. The constant for the exponential decay was determined from the material balance of the solute and proper boundary conditions. Their approximate expressions were later confirmed by Smith, et al. (3).

Smith, et al. (3) and Hulme (4) derived a theoretical expression for the case of diffusional mass transfer in the liquid without the assumptions used by Tiller, et al.

Wilcox (5) first studied the normal freezing of eutectic-forming organic systems. He successfully derived an expression for solute redistribution for an infinite charge with pure diffusional mass transfer in the liquid.

From a fluid-mechanical viewpoint, the solute rejected and accumulated near the freezing interface might be transported away from the interface not only by diffusion, but also by convection. In order to take this convective effect into account, Wagner (6) has suggested a boundary layer approach for the analysis of this problem. Here, he assumed that the solute moved purely by diffusion in a thin layer adjacent to the interface, and outside of this layer, complete mixing prevailed.

Burton, Prim, and Slichter (7) have derived an expression for solute redistribution for systems forming solid solutions based on this approach with a quasi-steady state assumption. For eutectic-forming systems, theoretical analysis has been made by Wilcox (5) using a similar approach.

In practice, the theoretical separations are seldom attained. Many workers (8,9,10) have observed this effect for normal freezing

and the related zone melting process. The failure of the theoretical analysis is thought to be due to interfacial instability called "constitutional subcooling," which causes the formation of a nonplanar interface. This phenomenon, first recognized by Chalmers (8), results in the trapping of liquid at the freezing interface and hence occlusion of liquid in the solid phase.

The major objective of this investigation was to obtain quantitative results on this subject. A brief quantitative analysis and experimental observations concerning this phenomenon are presented in Chapter IV and Chapter VI.

II. THEORETICAL DEVELOPMENT FOR MASS TRANSFER IN NORMAL FREEZING

A. Introduction

In the introductory chapter to this work, it was noted that the mixing condition in the liquid phase plays an important role in the segregation attained by normal freezing. In this chapter, the differential equations and boundary conditions for normal freezing are derived for both the case of pure diffusional mass transfer (no-mixing case) and the case of partial mixing (boundary layer approach). For the purpose of the present work, only solutions for eutectic-forming systems are presented.

B. Derivation of the Differential Equation, Boundary Conditions, and Solutions

The most convenient coordinate system for the analysis of this process is a moving coordinate system. Instead of a moving interface, the process is pictured as a steady bulk flow toward the interface. The interface is located at $z = 0$ with the positive z-axis extending into the liquid. The interfaces are assumed planar and the cross-section uniform, so that the problem becomes a one-dimensional one. Furthermore, the density and diffusivity are assumed to be independent of concentration and temperature, although the density may be different in the solid and liquid. Diffusion in the solid is assumed to be negligible. With these assumptions and the coordinate system, the equation of continuity for

the solute in the liquid phase becomes

$$D\frac{\partial^2 C}{\partial z^2} + \left(R_z \frac{\rho_s}{\rho_l}\right)\frac{\partial C}{\partial z} = \frac{\partial C}{\partial t} \qquad (2-1).$$

For simplicity in analysis, the following dimensionless groups are introduced.

$$\eta = \frac{zR_z}{D}\left(\frac{\rho_s}{\rho_l}\right)$$

$$\Phi = \frac{C}{C_o}$$

$$\tau = \frac{tR_z^2}{D}\left(\frac{\rho_s}{\rho_l}\right)$$

Substituting these expressions into equation (2-1), there is obtained:

$$\frac{\partial^2 \Phi}{\partial \eta^2} + \frac{\partial \Phi}{\partial \eta} = \frac{\partial \Phi}{\partial \tau} \qquad (2-2)$$

which is the desired differential equation governing diffusive mass transfer in normal freezing.*

Common Boundary Condition

Figure (2-1) shows the fluxes at the freezing solid-liquid interface. Making a material balance at the interface, there is obtained:

$$R_z(C - C_s) + D\frac{\partial C}{\partial z} = 0 \qquad \text{at } z = 0 \qquad (2-3).$$

Again substituting η, Φ and τ and letting $\Phi_s = C_s/C_o$, there results:

$$\frac{\partial \Phi}{\partial \eta} + (\Phi - \Phi_s) = 0 \qquad \text{at } \eta = 0 \qquad (2-4).$$

*This equation is valid also for the related process of zone melting.

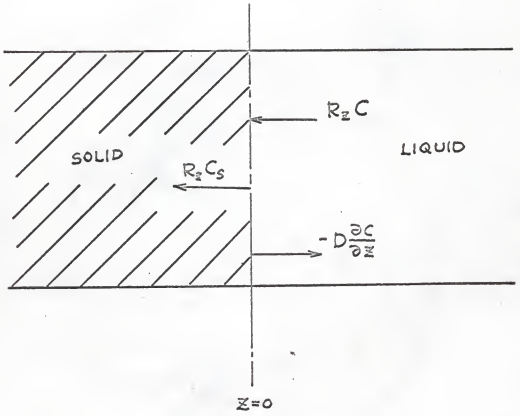

Fig. 2-1. MASS FLUXES AT FREEZING INTERFACE.

This boundary condition is common to both the boundary layer and the diffusion models.

Diffusion Model

Another boundary condition can be obtained under the assumption that the solute does not diffuse very far from the moving interface. Furthermore, if the amount of melt originally charged is very large compared with the freezing rate, the solute diffuses only a short distance into the liquid. This physical argument suggests

$$C = C_o \qquad \text{at } z = \infty \qquad (2 - 5)$$

or in dimensionless form

$$\bar{\varphi} = 1 \qquad \text{at } \eta = \infty \qquad (2 - 6).$$

In addition, the condition of uniform initial concentration gives the following initial condition:

$$C = C_o \qquad \text{at } t = 0 \qquad (2 - 7)$$

or written in dimensionless form,

$$\bar{\varphi} = 1 \qquad \text{at } \tau = 0 \qquad (2 - 8).$$

For eutectic-forming systems, two separate regimes must be recognized during the normal freezing process: (1) the liquid phase solute concentration at the interface is less than the eutectic composition, C_e, and the solid formed contains pure solvent only, (2) as more solid forms, the solute concentration of the liquid at the interface reaches the eutectic concentration and solute and solvent are deposited thereafter. For convenience in analysis, we refer to the first regime as the "Initial Period" and the second as the "Final Period."

The boundary conditions for the normal freezing of eutectic-forming

systems can now be stated:

(a) For the initial period, it is obvious that Φ_s equals zero. Hence, equation (2-3) becomes

$$\frac{\partial \Phi}{\partial \eta} = -\Phi \qquad \text{at } \eta = 0 \qquad (2-9).$$

(b) For the final period

$$\Phi = \frac{C_o}{C_o} \equiv \xi \qquad \text{at } \eta = 0$$

equation (2-3) becomes

$$\frac{\partial \Phi}{\partial \eta} = \Phi_s - \xi \qquad \text{at } \eta = 0 \qquad (2-10).$$

This means that until Φ at $\eta = 0$ reaches ξ, Φ_s is zero and Φ is calculated from equations (2-2), (2-9), (2-6), and (2-8) during the initial period.

Solution for the Initial Period

For the initial period, where $\Phi_s = 0$ and $\Phi_{\eta=0} < \xi$, the problem is, therefore, not to find the solute concentration in the solid, but to determine the duration of the initial period. The solution of equations (2-2), (2-6), (2-8), and (2-9) has been obtained by Wilcox (12) by means of Laplace Transformation and is:

$$\Phi = 1 - \tfrac{1}{2}\operatorname{erfc}\left(\frac{\eta + \tau}{2\sqrt{\tau}}\right) + \tfrac{1}{2}(1 - \eta + \tau)e^{-\eta}\operatorname{erfc}\left(\frac{\eta - \tau}{2\sqrt{\tau}}\right)$$

$$+ \sqrt{\frac{\tau}{\pi}} \exp\left\{-\eta - \left(\frac{\eta - \tau}{2\sqrt{\tau}}\right)^2\right\} \qquad (2-11).$$

Equation (2-11) gives the concentration of solute in the liquid as a function of time and distance from the interface. For the solid phase,

the composition profile is represented by

$$\Phi_s = 0 \qquad (2-12).$$

In order to predict the duration of the initial period, the concentration at the freezing interface is required. This is found by setting η equal to zero in equation (2-11) to obtain:

$$\Phi_{\eta=0} = \frac{2+\tau}{2}\left(1 + \operatorname{erf}\sqrt{\frac{\tau}{2}}\right) + \sqrt{\frac{\tau}{\pi}}\, e^{-\tau/4} \qquad (2-13).$$

The initial period persists until the liquid concentration at the interface reaches the eutectic composition. Thus, the duration of the initial period τ_o can be obtained by setting $\Phi_{\eta=0} = \xi$ in equation (2-13).

$$\xi = \frac{2+\tau_o}{2}\left(1 + \operatorname{erf}\sqrt{\frac{\tau_o}{2}}\right) + \sqrt{\frac{\tau_o}{\pi}}\, e^{-\tau_o/4} \qquad (2-14)$$

The total length of solid frozen without any impurity can be determined from τ_o.

$$Z_o = \frac{\tau_o D}{R_z}\left(\frac{\rho_l}{\rho_s}\right)^2 \qquad (2-15)$$

The duration of initial period, calculated from equation (2-14) for various ξ, is shown in Figure (2-2). Because equation (2-14) is rather unwieldy, it is of interest to find a limiting form for large values of τ. If we let $\tau \to \infty$, equation (2-11) simplifies to

$$\Phi = 1 + (1 + \tau - \eta)e^{-\eta} \qquad (2-16)$$

and equation (2-14) becomes

$$\Phi_{\eta=0} = \xi = 2 + \tau_o \qquad (2-17).$$

Wilcox (12) has shown that equations (2-16) and (2-17) are valid for τ (or τ_o) greater than 5 with an error less than 2%.

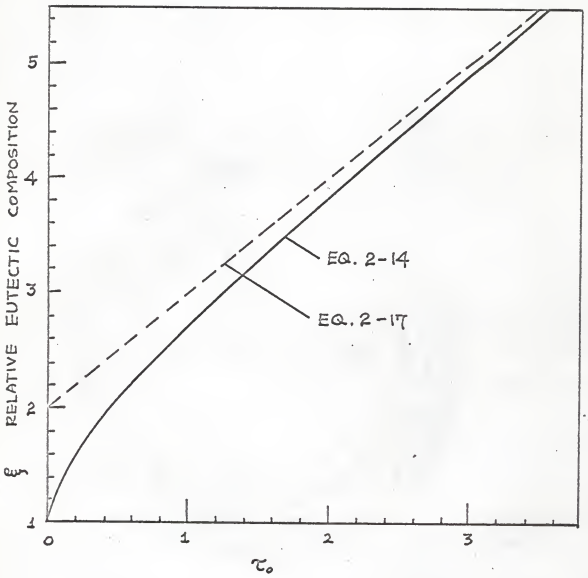

Fig. 2-2 THE DURATION OF INITIAL PERIOD FOR DIFFUSION MODEL.

From Figure (2-2), we see that τ_o increases with increasing ξ. Recalling the definitions of these quantities,

$$\tau_o = \frac{t_o R_z^2}{D}\left(\frac{\rho_s}{\rho_l}\right)^2 \quad \text{or} \quad t_o R_z\left(\frac{\rho_s}{\rho_l}\right) = \frac{\tau_o D}{R_z\left(\frac{\rho_s}{\rho_l}\right)}$$

$$\xi = \frac{C_e}{C_o}$$

we note that for a given system (a fixed C_e), the amount of pure material obtained (which is proportional to $t_o R_z$) decreases with increasing initial concentration, C_o, and increasing freezing rate.

Solution for the Final Period

When $\phi_{\eta=0} = \xi$, equations (2-2), (2-6) and (2-10) describe the solute concentrations in the solid and liquid phases. In addition, an "initial condition" for $\tau = \tau_o$ is given by equation (2-11), the solution from the initial period. This problem has also been solved by Wilcox (12); the solution is given for the liquid phase as:

$$\phi = 1 + (\tau_t - \eta + \xi - 1)e^{-\eta} + \tfrac{1}{2}\left\{-\eta(1 - e^{-\eta}) - \tau_t(1 + e^{-\eta}) + (\tau_t - \eta)e^{-\eta}\operatorname{erf}\left[\frac{\eta - \tau_t}{2\sqrt{\tau_t}}\right] + (\tau_t + \eta)\operatorname{erf}\left[\frac{\eta + \tau_t}{2\sqrt{\tau_t}}\right]\right\} \qquad (2-18)$$

and for the solid phase as

$$\phi_s = -\frac{\tau_t}{2} + \frac{\tau_t + 2}{2}\operatorname{erf}\frac{\sqrt{\tau_t}}{2} + \sqrt{\frac{\tau_t}{\pi}}\, e^{-\tau_t/4} \qquad (2-19)$$

where τ_t is the dimensionless time from beginning of terminal period, $\tau_t = (\tau - \tau_o)$.

During the final period, the solute concentration in the solid

is increasing; and after sufficient time has elapsed, a steady state condition will be reached where the solute concentration in the solid asymptotically approaches C_o. This is dictated by the assumption of an infinite quantity of liquid, for when the process is viewed as a flow toward the interface, it will be recognized that material balance considerations require this steady state condition. In other words, after sufficient time, the flow of solute toward the interface must equal the flow of solute away from the interface, i.e. $\Phi_s = 1$.

It is easily confirmed that as τ_t tends to infinity, equation (2-18) and equation (2-19) approach the steady state solution:

$$\bar{\Phi} = 1 + (\xi - 1)e^{-\eta}$$

and $$\Phi_s = 1 \ .$$

A sketch of a solid composition profile illustrating the initial, final and steady state periods is presented in Figure (2-3).

Boundary-Layer Model

Needless to say, pure diffusional mass transfer is seldom realized in a fluid because of the convective effect due to temperature and/or density differences in the liquid phase. If convection is negligible, the solution obtained in the previous section is valid. However, when convection occurs in the liquid phase, it is necessary to develop another mechanism, taking into consideration both convection and diffusion. A boundary layer approach has been suggested by Wagner (6), in which he assumed that inside the boundary layer, mass transfer is by diffusion only, while outside it, complete mixing prevails.

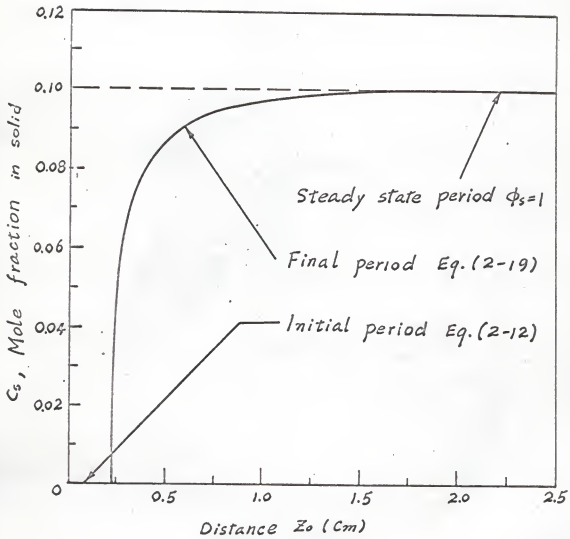

Fig. 2-3 Concentration profile in the solid for normal freezing with diffusion model for $\frac{R}{V} = 4$ and $R_{Z/D} = 5$ cm. (12)

Quasi-Steady State Solutions

Inside the boundary layer, the solute continuity equation, equation (2-2), applies.

On the outer edge of the boundary layer, $\eta = \frac{\delta R_z}{D}\left(\frac{\rho_s}{\rho_1}\right) \equiv b$, it is assumed that convection insures the uniformity of bulk liquid concentration. Stated mathematically:

$$\phi = \phi_b \equiv \frac{C_b}{C_o} \qquad \text{at } \eta = b \qquad (2 - 20).$$

The initial condition, equation (2-8), and the boundary condition at $\eta = 0$, equation (2-4), remain unchanged.

With this idealized mechanism, the solution for prediction of segregation in normal freezing has been obtained by Wilcox (5) for eutectic systems under a quasi-steady state consideration, assuming the solute contained within the boundary layer to be negligible in comparison with that of the bulk liquid. That is, after a very short transient period, the rate of change of solute concentration within the boundary layer, $\frac{\partial C}{\partial t}$, is small in comparison to the flow of solute through the boundary layer. Under this quasi-steady state assumption, the continuity equation (2-2) becomes

$$\frac{d^2\phi}{d\eta^2} + \frac{d\phi}{d\eta} = 0 \qquad (2 - 21).$$

As noted previously, the concentration profiles resulting from the normal freezing of eutectic-forming mixtures have two regions. These are discussed separately.

1. For the initial period in which pure solvent freezes out, equations (2-21), (2-20) and (2-9) yield the solution:

$$\Phi = \Phi_b \frac{e^{-\eta}}{e^{-b}} \qquad \text{for } 0 \leq \eta \leq b \qquad (2-22)$$

and $$\Phi = \Phi_b \qquad \text{for } b \leq \eta \qquad (2-23).$$

The duration of the initial period can be calculated by setting $\Phi_{\eta=0} = \xi$ in equation (2-21) to obtain

$$\Phi_b = \xi e^{-b} \quad .$$

Neglecting the solute contained in the boundary layer, a solute material balance gives

$$\frac{d g_o}{1 - g_o} = \frac{d \Phi_b}{1 - \Phi_b} \quad .$$

or $$g_o = 1 - \frac{1}{\xi e^{-b}} \qquad (2-24)$$

where g_o is the fraction frozen during the initial period.

For an estimation of g_o, a plot based on equation (2-24) is shown in Figure (2-4) which gives the value of g_o for various values of ξ and b. Recalling the definitions of ξ and b

$$\xi = \frac{C_e}{C_o}$$

$$b = \frac{\delta R_z}{D} \left(\frac{\rho_s}{\rho_l}\right)$$

from Figure (2-4), one again observes that for a given system (fixed values of C_e, ρ_e, ρ_s, and D), higher solute concentration (C_o) and freezing rate (R_z) produce lower yields of pure solvent (g_o).

2. For the final period in which solute appears in the solid phase, no solution has been obtained by means of the boundary layer approach. However, for the usual normal freezing, ξ is large due to

dilute solutions originally charged and b is small because of the low freezing rate. Under these conditions, it is seen from Figure (2-4) that the initial period is quite large, i.e. the final period is small and becomes unimportant. For example, if $\xi = 30$, and $b = 1$, the initial period persists until the charge is 91% frozen. Therefore, neglecting the consideration of this short period is of no serious practical consequence.

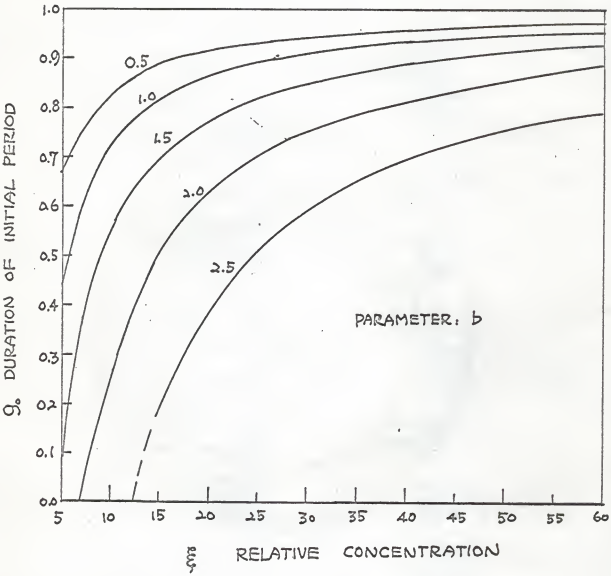

Fig. 2-4. THE DURATION OF INITIAL PERIOD FOR BOUNDARY-LAYER MODEL.

III. COMPUTER SOLUTION FOR SOLUTE REDISTRIBUTION BY THE BOUNDARY LAYER APPROACH

A. Introduction

The solute redistribution in normal freezing by the boundary layer approach has been derived in the last chapter under a quasi-steady state approximation, in which the overall material balance has been made by assuming the size of the boundary layer was negligible and that it contains an insignificant amount of impurity. However, as was pointed out by Chalmers (13), the boundary layer thickness for natural convection lies in the order of magnitude of 10^{-1} cm. Therefore, the accuracy of quasi-steady state solution becomes poor when the amount of initial melt is small.

Another deficiency of the quasi-steady state approximation is the absence of an initial transient period. Wilcox (1) has suggested an analytical solution for this unsteady state period by assuming the initial transient to be the period in which the concentration at the outer edge of the boundary layer remains the same as that of the original charge, C_o. In other words, when the concentration in the bulk C_b becomes greater than C_o, the transient period stops and the quasi-steady state solution becomes valid thereafter. From a physical viewpoint, this assumption seems over-simplified. In fact, a more precise boundary condition at the outer edge of the boundary layer must be obtained in order to solve this problem without losing the physical significance. Without this new boundary condition, the exact solution from equations

(2-2), (2-4), (2-19) and (2-8) can not, in general, be obtained analytically or even numerically.

B. Derivation of the Boundary Condition

Considering the material balance at the outer edge of the boundary layer, it is apparent that the mass flux diffusing out of the boundary layer is $-D \left.\frac{\partial C}{\partial z}\right|_{z=\delta}$. Hence, the total mass diffusing out of the boundary layer per unit time is $-DA \left.\frac{\partial C}{\partial z}\right|_{z=\delta}$, where A is the cross-sectional area of the tube. By the boundary layer approach, the solute diffusing out will be completely mixed and uniformly distributed in the bulk liquid. A solute material balance yields

$$-DA \left.\frac{\partial C}{\partial z}\right|_{z=\delta} = (1 - \delta - R_z t)A \frac{dC_b}{dt} \qquad (3 - 1)$$

or expressed in dimensionless form

$$\frac{d\Phi_b}{dt} = \frac{\left.\frac{\partial \Phi}{\partial \eta}\right|_{\eta=b}}{L - b - \tau} \qquad (3 - 2).$$

Integration of equation (3-2) yields

$$\Phi_b = a - \int_0^\tau \frac{\left.\frac{\partial \Phi}{\partial \eta}\right|_{\eta=b}}{L - b - \tau} d\tau \qquad (3 - 3)$$

where "a" is the integration constant and is evaluated from the following boundary condition. When $\tau = 0$, $\Phi_b = 1$, this implies that $a = 1$. Substituting the expression for Φ_b in equation (2-20) gives

$$\Phi = 1 - \int_0^\tau \frac{\left(\frac{\partial \Phi}{\partial \eta}\right)_{\eta=b}}{L - b - \tau} d\tau \qquad \text{at } \eta = b \qquad (3 - 4).$$

C. Solid Solution Systems with Constant Distribution Coefficient

Equations (2-2), (2-4), (3-4) and (2-8) will be sufficient to define this problem. Unfortunately, no analytical solution has been derived as yet. However, a numerical solution by means of finite difference is presented here.

In finite difference form, $\frac{\partial \Phi}{\partial \tau}$, $\frac{\partial \Phi}{\partial \eta}$ and $\frac{\partial^2 \Phi}{\partial \eta^2}$ will take the forms (14).

$$\frac{\Phi_{i,j+1} - \Phi_{i,j}}{\Delta\tau}$$

$$\frac{\Phi_{i+1,j} - \Phi_{i-1,j}}{2\Delta\eta}$$

$$\frac{\Phi_{i+1,j} - 2\Phi_{i,j} + \Phi_{i-1,j}}{(\Delta\eta)^2}$$

Here, $\Delta\tau$ is an interval in τ, and $\Delta\eta$ in η; j is the number of the step along the τ-axis; i the step number along the η-axis.

The truncational error for $\frac{\partial^2 \Phi}{\partial \eta^2}$ and $\frac{\partial \Phi}{\partial \eta}$ by taking the finite difference forms are $\frac{\Delta\eta^2}{12}$ and $\frac{\Delta\eta^2}{6}$ respectively, and that for $\frac{\partial \Phi}{\partial \tau}$ is $\frac{\Delta\tau}{2}$. Therefore, for the finite difference equation to be convergent, the following condition must be satisfied:

$$\frac{\Delta\eta^2}{12} + \frac{\Delta\eta^2}{6} = \frac{\Delta\tau}{2}$$

or

$$\frac{\Delta\eta^2}{\Delta\tau} = 2 \ .$$

This mesh ratio happens to be the same as Landau (14) used in his finite difference solution of normal freezing under diffusion model.

Then, the finite-difference equation corresponding to the governing

differential equation (2-2) becomes

$$\Phi_{i,j+1} = (\tfrac{1}{2} + \frac{\Delta\tau}{2\Delta\eta})\Phi_{i+1,j} + (\tfrac{1}{2} - \frac{\Delta\tau}{2\Delta\eta})\Phi_{i-1,j} \qquad (3-5).$$

Equation (2-4) becomes

$$\frac{1}{2\Delta\eta}(\Phi_{+1,j} - \Phi_{-1,j}) + \frac{\Phi_{+1,j} + \Phi_{-1,j}}{2}(1 - K_o) = 0$$

where $\Phi(-1,j)$ represents the hypothetical point outside the interface, or

$$\Phi_{-1,j} = \frac{1 + (1 - K_o)\Delta\eta}{1 - (1 - K_o)\Delta\eta}\Phi_{1,j} \qquad (3-6).$$

The initial condition is

$$\Phi(i,o) = 1 \quad \text{for all } j \qquad (3-7).$$

The boundary condition outside the boundary layer, equation (3-2), can be expressed as

$$\frac{\Phi_{\Delta,j+1} - \Phi_{\Delta,j}}{\Delta\tau} = \frac{\Phi_{\Delta-1,j} - \Phi_{\Delta,j}}{\Delta\eta} \cdot \frac{1}{L - b - \tau}$$

or

$$\Phi_{\Delta,j+1} = \frac{\Phi_{\Delta-1,j} - \Phi_{\Delta,j}}{L\frac{\Delta\eta}{\Delta\tau} - b\frac{\Delta\eta}{\Delta\tau} - j\Delta\eta} + \Phi_{\Delta,j} \qquad (3-8)$$

where $\Phi(\Delta,j)$ is the point on the edge of boundary layer and $\Phi(o,j)$ on the interface.

Equation (3-8) can be rewritten as

$$\Phi_{\Delta,j+1} = \frac{\Phi_{\Delta-1,j} - \Phi_{\Delta,j}}{b\frac{\Delta\eta}{\Delta\tau}(\frac{1}{\delta} - 1) - j(\Delta\eta)} + \Phi_{\Delta,j} \qquad (3-9).$$

In carrying out a solution, we divide the boundary layer thickness, b, into Δ equal intervals and initially set Φ equal to 1.0 over the entire interval of the boundary layer as stated in equation (3-7). The values of $\Phi_{i,j}$ inside the boundary layer, where mass transfer occurs by diffusion only, were calculated by equation (3-5), except for the two end points $\Phi(-1,j)$ and $\Phi(\Delta,j)$ which will be obtained by equations (3-6) and (3-9).

This process was repeated until j reached the value by which the denominator of equation (3-9) approached zero, i.e. the liquid originally charged was solidified except for a small amount which was essentially the length of the boundary layer. Φ_s can be obtained from the relation that $\Phi_s = K_o\Phi(o,j)$ at each j.

Calculations were made for $K_o = 0.2$ and 0.02 and for b = 1, 2 and 5. It was found necessary, in general, to make $\Delta\eta$ approximately 0.05 and $\Delta\tau = 0.00125$, or to make $\Delta\eta$ smaller and keep the ratio $\frac{(\Delta\eta)^2}{\Delta\tau}$ equal to 2.

It is clearly shown in equation (3-9) that, in addition to the parameters b and K_o, the parameter $1/\delta$ will also affect the concentration profile in the liquid phase, and hence, the segregation curve, Φ_s. As was pointed out by Chalmer (13), the boundary layer thickness for natural convection lies in the order of magnitude 0.1 cm. Our calculations are, therefore, based on $1/\delta = 100$ and 50, which is equivalent to a total amount of charge of the order of magnitude of 10 cm. for normal freezing.

Generally speaking, a correct solution to any mass transfer problem must satisfy an overall material balance. For the case of normal freezing, this means that the area between $\Phi_o = 1.0$ and the Φ_s curve must equal the area between $\Phi_o = 1$ and the Φ ourve (see Figure 3-1).

This can be written analytically:

$$\int_0^{\tau} (1 - \Phi_s)d\tau = \int_0^{1-\tau/L} (\Phi - 1)d\eta \qquad (3 - 10).$$

It was found that the computer solution described above did satisfy this condition for all cases investigated.

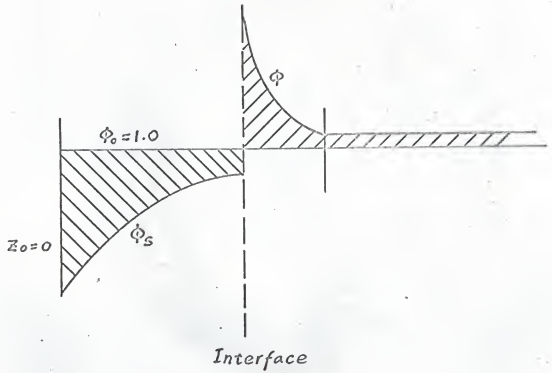

Fig. 3-1 Concentration profile in solid and liquid phase showing material balance for boundary layer approach.

D. Simple Eutectic-Forming Systems

It is clearly shown in Figure (2-4) that the final period is unimportant for the usual normal freezing of eutectic-forming systems. Therefore, only the initial period is discussed here.

During the initial period, no solute is incorporated in the freezing solid. Hence, we may simply set K_o equal to zero in the previous calculations.

E. Results and Discussions

Solid Solution System

The liquid phase concentration profiles calculated by the finite difference method for a sample value of K_o, b, and $1/\delta$ is presented in Figure (3-2). The quasi-steady state solution is also plotted for comparison. The corresponding solid phase concentration profiles are shown in Figure (3-3).

In those figures, the fraction frozen, g, was obtained from the following relation:

$$\tau = \frac{tR_z^2}{D}\left(\frac{\rho_s}{\rho_l}\right)^2 = \left\{\frac{tR_z}{l}\left(\frac{\rho_s}{\rho_l}\right)\right\} \cdot \left\{\left(\frac{lR_z}{D}\right)\left(\frac{\rho_s}{\rho_l}\right)\right\}$$

or $$\tau = gL \qquad (3-11).$$

Figures (3-4) and (3-5) summarize the results of calculations for K_o equal to 0.2 and 0.02 respectively. It can be seen in these figures that the quasi-steady state solution is acceptable if the dimensionless boundary layer, b, is small and the value of $1/\delta$ is large, which is the usual case in normal freezing. This is due to the fact that the amount

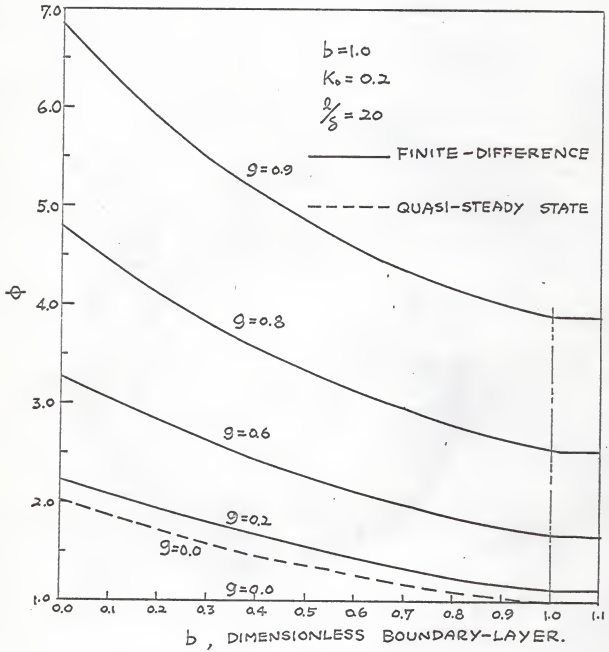

Fig. 3-2. TYPICAL CONCENTRATION PROFILE IN THE LIQUID PHASE OBTAINED BY FINITE-DIFFERENCE CALCULATION.

of solute accumulated in the boundary layer is negligible compared with that in the bulk liquid when the fraction frozen is small. But the amount of solute accumulated in the boundary layer is relatively more significant when the fraction frozen becomes large. Therefore, the neglect of this quantity in the material balance would result in large deviations from the exact solution obtained by finite-difference calculation. For instance, in Figure (3-3), the deviation at $g = 0.1$ is 4.8%, while at $g = 0.8$, the deviation is 13.6%.

Another obvious failing of the quasi-steady state approach is the neglect of a transient period. In fact, the solid initially frozen out should follow a short transient period before the quasi-steady state results would be valid. In any case, it is quite obvious that the concentration of the solid initially frozen out predicted by the quasi-steady state solution is K_E instead of K_o as it should be, when considering an initially uniform liquid and a constant distribution coefficient. This deviation is clearly shown in Figures (3-3), (3-4), and (3-5).

Wilcox (1) has derived an equation to correct this deviation. However, his correction is based on an over-simplified assumption and would not be valid when the value of b is large (high freezing rate). A typical comparison between his solution and the finite-difference calculation is shown in Figure (3-6). Wilcox's solution seems consistent with the finite-difference calculation up to $g = 0.1$ for the case where $1/\delta$ is very small. In Figures (3-4) and (3-5), concentration profiles in the solid phase obtained by three methods for various values of K_o, $1/\delta$ and b are plotted. It is clearly seen that in some cases Wilcox's solution is valid only in a very short initial period and in some other cases, e.g. in the case $K_o = 0.2$ and $b = 5$, it is not valid.

Simple Eutectic-Forming Systems

For eutectic-forming systems, the comparison between the quasi-steady state solution and the exact solution obtained by the finite-difference calculation applies only to the initial period. Figure (3-7) shows the results obtained by both methods as well as applying Wilcox's solution to eutectic systems under different dimensionless freezing rates. In similarity to the solid solution systems, it shows that for higher freezing rates and smaller charges (smaller l), the approximation of the quasi-steady state solution becomes poor. For example, when $1/\delta = 50$, $b = 2.5$ and an original concentration of one tenth of the eutectic concentration, the quasi-steady state solution predicts no pure solid formed, while the finite-difference calculation shows that 10 per cent of the charge is obtained pure. It is clearly shown that Wilcox's solution is valid only in a very short initial period for the case of $b = 1$, and again is not valid for b greater than 2.

F. Conclusion

All results of the finite-difference calculation show that the accuracy of the quasi-steady state depends on whether the amount of solute accumulated in the boundary layer is significant. Therefore, the question of whether the initial transient period is important depends on the freezing rate, distribution coefficient, and the length of the charge. It is concluded that when the values of K_o (in solid solution systems) and $1/\delta$ are small and the solidification is carried out at a sufficiently high freezing rate, the approximation of the quasi-steady state solutions becomes poor. However, for ordinary normal freezing,

the values of $1/\delta$ lie in the order of magnitude of 1×10^2, and the freezing rate is very low. The quasi-steady state approximation is, therefore, applicable without serious error.

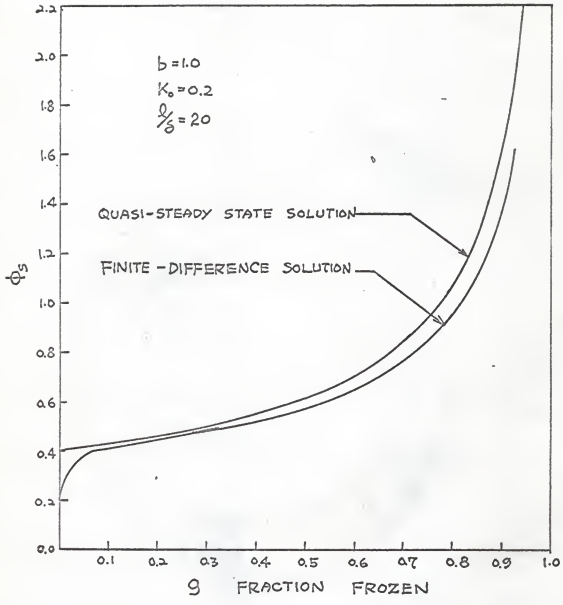

Fig. 3-3. TYPICAL CONCENTRATION PROFILE IN SOLID PHASE OBTAINED BY FINITE-DIFFERENCE CALCULATION.

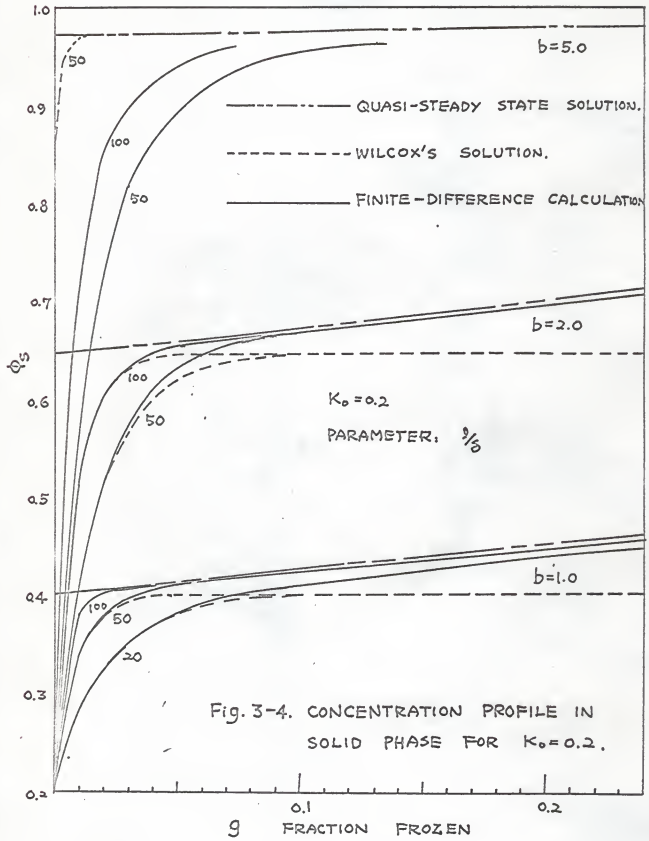

Fig. 3-4. CONCENTRATION PROFILE IN SOLID PHASE FOR $K_o = 0.2$.

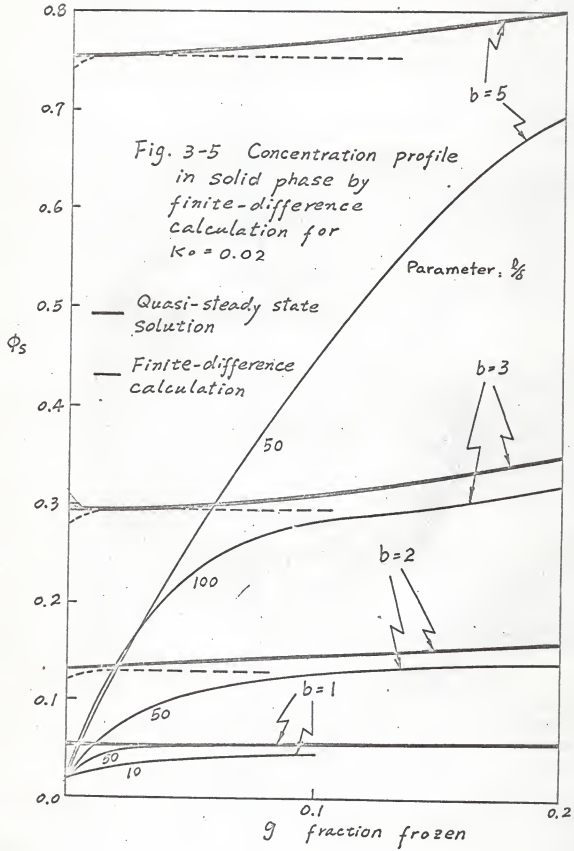

Fig. 3-5 Concentration profile in solid phase by finite-difference calculation for $K_0 = 0.02$

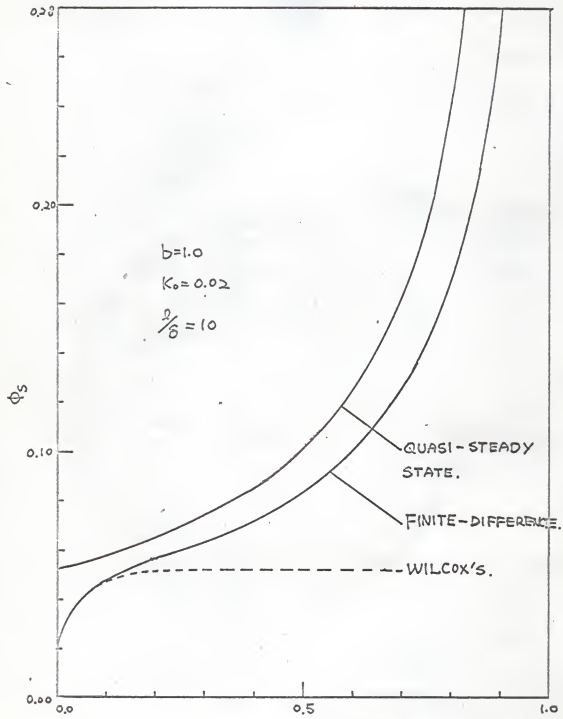

Fig. 3-6. A COMPARISON BETWEEN WILCOX'S SOLUTION AND FINITE-DIFFERENCE CALCULATION.

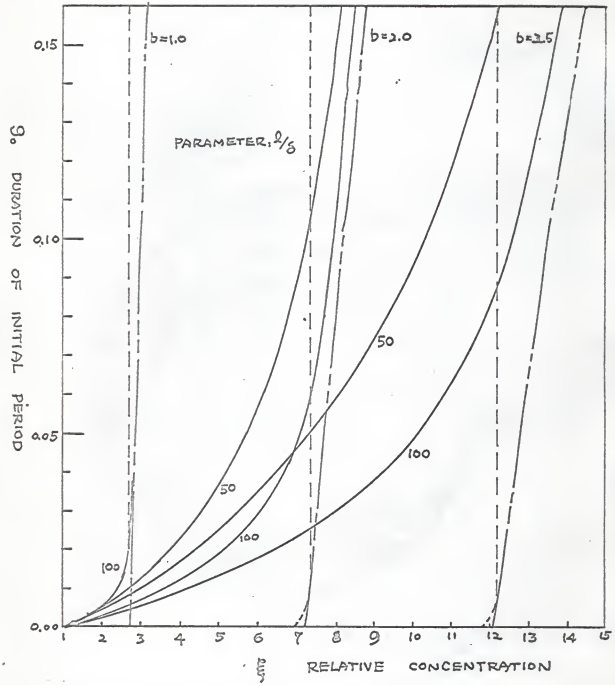

Fig. 3-7. COMPARISON BETWEEN QUASI-STEADY STATE AND FINITE-DIFFERENCE SOLUTIONS FOR SIMPLE EUTECTIC SYSTEM.

IV. THERMAL CONSIDERATIONS AND CONSTITUTIONAL SUBCOOLING IN NORMAL FREEZING

A. Instruction

Of the assumptions made in obtaining the foregoing solutions to solute redistribution problems, the assumption of a planar freezing interface is the most troublesome. When a solution undergoes a normal freezing process, the liquid in contact with the advancing solid-liquid interface will, in general, have a composition higher than that of the bulk liquid ($K_o < 1$). Hence, the liquidus temperature of the liquid in contact with the interface is lower than that of the liquid at a greater distance from the interface. In other words, the liquidus temperature of the bulk liquid becomes higher than that of the interface, and possibly exceeds the imposed temperature adjacent to the interface (see Figure 4-1). When this condition occurs, there will be a region ahead of the interface in which there is a greater thermal driving force than exists at the interface, and thus the planar interface becomes unstable. Two manifestations of this instability have been proposed:

(1) According to Landau (19), a layer of subcooled liquid rapidly freezes, entrapping solute. This is a cyclic process which repeats itself when sufficient subcooling is again established.

(2) Because of the subcooling, any protuberence on the interface will tend to grow ahead of the interface. Chalmers (13) has shown that this leads to a cellular structure with spaces between cells where liquid may become trapped. This type of interfacial structure

has been observed in metallurgical systems.

In both cases, the instability occurs only if the T and T_E curves in Figure (4-1) intersect. Hence, the condition for stability of the planar interface is

$$\left.\frac{dT_E}{dz}\right|_{z=0} \leq \left.\frac{dT}{dz}\right|_{z=0} \qquad (4-1).$$

Equations based on this condition have been remarkably successful in predicting the onset of the non-planar interfacial structure for systems forming solid solutions.

Various equations based on this stability criterion are derived for both diffusion and boundary-layer models in the following sections. Experimental results have been obtained and are presented and discussed in Chapter VI.

B. Imposed Temperature Profile in the Liquid Phase

Assumptions

The following assumptions were made in order to simplify the problem. They are listed here for convenience, although some are discussed later, in Chapter VI.

(a) The temperature profile is a function of z only, although radial heat transfer has been considered by means of heat input from the surrounding.

(b) The freezing interface is planar.

(c) Natural convection in the liquid phase is negligible.

(d) The solid-liquid interface is at its equilibrium temperature.

(e) The heat transfer coefficient from the tube to the surrounding

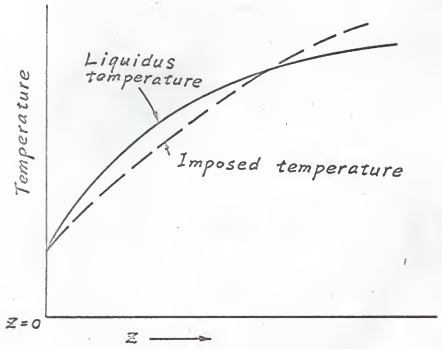

Fig. 4-1 Schematic diagram of constitutional subcooling.

air is constant.

(f) For the low freezing rate used in normal freezing, a quasi-steady state treatment suffices for our purpose.

(g) The temperature of ambient air surrounding the tube is constant.

Derivation of the Governing Differential Equation and the Boundary Conditions

By using the foregoing assumptions, the differential equations governing heat transfer in the liquid phase may be derived (5). A heat balance over a differential element, as shown in Figure (4-2), yields:

$$-k\left(\frac{dT}{dz}\right)_{z+\Delta z}\pi R^2 + R_z\rho_l C_p T_{z+\Delta z}\pi R^2$$
$$= h(T_z - T_a)2\pi R\Delta z - k\left(\frac{dT}{dz}\right)_z \pi R^2 + R_z\rho_l C_p T_z \pi R^2 \qquad (4-2).$$

Dividing through by $k\pi R^2\Delta z$ and taking the limit as $\Delta z \to 0$, we obtain the differential equation

$$\alpha\frac{d^2T}{dz^2} + R_z\frac{dT}{dz} - \beta(T - T_a) = 0 \qquad (4-3)$$

where $\beta = \dfrac{2h}{R\rho_l C_p}$ and $\alpha = \dfrac{k}{\rho_l C_p}$.

The boundary conditions necessary for a complete solution are as follows:

(a) As $z \to \infty$, $T_a \to T_R$ and $T \to T_R$, i.e. the temperatures for both liquid in the tube and the ambient air surrounding the tube at a distance far from the freezing interface approach the steady room temperature.

(b) At $z = 0$, $T = T_e$, i.e. at the interface, the temperature is the liquidus temperature of the solution at the interface.

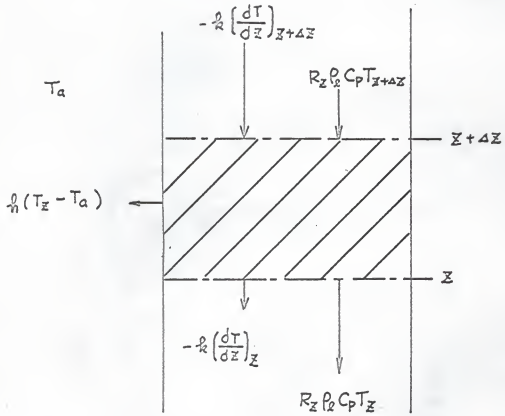

Fig. 4-2. DIFFERENTIAL ELEMENT OF LIQUID, SHOWING HEAT FLUXES.

Solution

The homogeneous part of equation (4-3) gives the general solution of the form of

$$T = a_1 \exp\left(\frac{-R_z + \sqrt{R_z^2 + 4\alpha\beta}}{2\alpha} z\right) + a_2 \exp\left(\frac{-R_z - \sqrt{R_z^2 + 4\alpha\beta}}{2\alpha} z\right) .$$

A particular solution of equation (4-3) is

$$T = T_a .$$

Therefore, the solution to equation (4-3) is

$$T = a_1 \exp\left(\frac{-R_z + \sqrt{R_z^2 + 4\alpha\beta}}{2\alpha} z\right) + a_2 \exp\left(\frac{-R_z - \sqrt{R_z^2 + 4\alpha\beta}}{2\alpha} z\right) + T_a .$$

Boundary conditions (a) and (b) give

$$a_1 = 0 \qquad a_2 = (T_e - T_a)$$

Therefore, the desired temperature profile may be expressed as

$$T = (T_e - T_a) \exp\left(-\frac{R_z + \sqrt{R_z + 4\alpha\beta}}{2\alpha} z\right) + T_a$$

or, in dimensionless form

$$\frac{T - T_a}{T_e - T_a} = \exp\left(-\frac{R_z + \sqrt{R_z + 4\alpha\beta}}{2\alpha} z\right) \qquad (4 - 4).$$

C. The Liquidus Temperature Profile

If m is the slope of the liquidus line, $m = \frac{dT_E}{dC}$, and T_o is the freezing point of the pure solvent, then the following should represent equilibrium temperatures for dilute solutions:

$$T_E = T_o - mC \qquad (4 - 5)$$

where we take the value of m to be positive.

Diffusion Model

Substituting the expression for C as given by equation (3-11) into equation (4-5) gives the liquidus temperature profile:

$$T_E = T_o - mC_o\left[1 - \tfrac{1}{2}\mathrm{erf}\left(\frac{\eta+\tau}{2\sqrt{\tau}}\right) + \tfrac{1}{2}(1-\eta+\tau)e^{-\eta}\mathrm{erfc}\left(\frac{\eta-\tau}{2\sqrt{\tau}}\right) + \sqrt{\frac{\tau}{\pi}}\exp\left\{-\eta - \left(\frac{\eta-\tau}{\sqrt{\pi}}\right)^2\right\}\right] \qquad (4-6).$$

Boundary-Layer Model

Similarly, if the C in equation (4-5) is eliminated by means of equation (3-22), the liquidus temperature profile for this model is

$$T_E = T_o - mC_o\frac{e^{-\eta}}{e^{-b}} \qquad (4-7).$$

If we make an overall material balance by neglecting the solute contained in the boundary layer during the initial period, we obtain

$$C_b = \frac{C_o}{1-\varepsilon_p} \qquad (4-8).$$

Elimination of C_b between equations (4-8) and (4-7) gives

$$T_E = T_o - \frac{mC_o e^{-\eta}}{(1-\varepsilon_p)e^{-b}} \qquad (4-9).$$

D. Incubation Distance for the Occurrence of Constitutional Subcooling

Since constitutional subcooling can not exist until an enriched boundary layer has formed, it follows that cells should not form immediately when solidification begins, even if uniform values of $\frac{dT}{dz}$ and R_z are immediately established. The critical condition will not occur

until the initial transient has reached the stage at which the concentration gradient at the interface has a value such that the gradient of the equilibrium temperature exceeds that of the imposed temperature as expressed in equation (4-1). It follows that there must be an "incubation distance" for the occurrence of constitutional subcooling. It can be derived by substituting expressions for T_E and T into equation (4-1).

Diffusion Model

Substituting the expressions of T_E and T from equations (4-6) and (4-4), respectively, in equation (4-1), there is obtained:

$$\frac{mC_o R}{D}\left\{\sqrt{\frac{\tau}{\pi}}\, e^{-\tau/4} + \frac{2+\tau}{2}\left(1 + \operatorname{erf}\sqrt{\frac{\tau}{2}}\right)\right\}$$

$$= (T_a - T_e)\,\frac{R_z + \sqrt{R_z^2 + 4\alpha\beta}}{2\alpha} \equiv G \qquad (4-10)$$

or

$$\frac{DG}{mC_o R_z} = F(\tau) \qquad (4-11)$$

where $F(\tau)$ is defined as

$$F(\tau) = \sqrt{\frac{\tau}{\pi}}\, e^{-\tau/4} + \frac{2+\tau}{2}\left(1 + \operatorname{erf}\sqrt{\frac{\tau}{2}}\right).$$

A plot of $\frac{DG}{mC_o R_z}$ vs. τ is given in Figure (4-3). The incubation period is expressed as the time elapsed since the start of freezing.

Boundary-Layer Model

In equation (4-1), substituting the expressions for T_E and T from equations (4-9) and (4-4), it is found

$$\frac{DG}{mC_o R_z} = \frac{e^b}{1 - g_p} \qquad (4-12)$$

where g_p is the fraction frozen at the onset of subcooling.

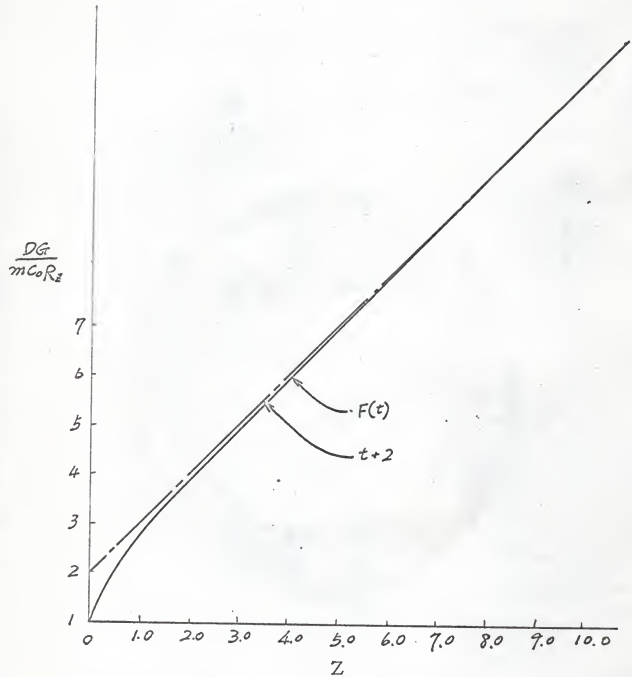

Fig. 4-3 Indication of incubation distance for diffusion model.

A plot of $\frac{DG}{mC_o R_z}$ vs. $\frac{1}{1 - \varepsilon_p}$ on log-log paper, shown in Figure (4-4), gives straight lines with unit slope.

Notice that all systems following the diffusion model could be correlated with a single relationship, whereas an adjustable parameter appearing in the boundary-layer model allows for different behavior among otherwise similar systems.

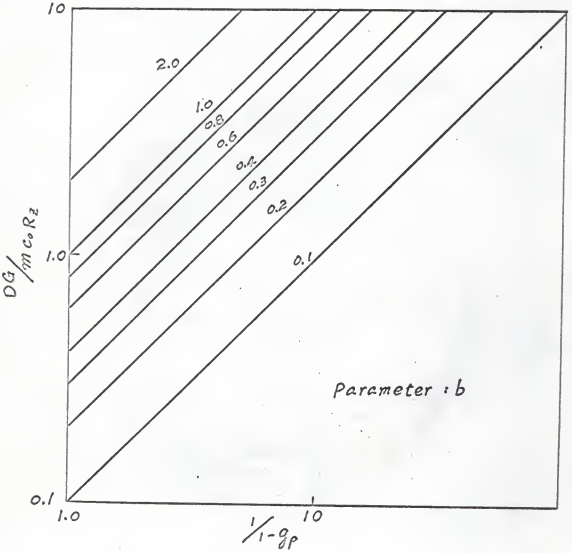

Fig. 4-4 Indication of incubation distance for boundary-layer model.

V. EXPERIMENTAL EQUIPMENT, PROCEDURE AND SYSTEMS

A. General Description of Equipment

The apparatus used for conducting normal freezing experiments consisted of a refrigerated methyl alcohol bath and a drive mechanism to control the freezing rate. The bath temperature was controlled and kept approximately at $-5^{\circ}C$ for all runs, with the maximum variation less than $\pm$ 0.1°C. To keep the bath at a uniform temperature, it was agitated by a 1/12 H.P. Fultork Labmotor operating a stirrer.

The drive mechanism was essentially an electric clockmotor located approximately 1 meter above the bath (see Figure 5-1). Spindles of different sizes ($\frac{3}{8}$" to 1" diameter) could be attached to the shaft of the clockmotor in order to vary the freezing rate.

A thin thread, connected to the glass tube containing the charge, was tied and wound several turns on the spindle. The spindle rotated at a constant rate of one revolution per 12 hours. Hence, the tube would descend at a constant rate in the ranges of 0.065 to 0.25 inch per hour, depending on the selected size of the spindle.

Temperature was measured by a copper-constantan thermocouple fabricated from 0.002 inch diameter wire and suspended in the liquid at a fixed position relative to the tube. As freezing progressed and the solid-liquid interface moved toward the thermocouple, readings were recorded at definite times so that the relative position of the thermocouple could be determined from the known freezing rate. The time at which the thermocouple touched the interface was also recorded.

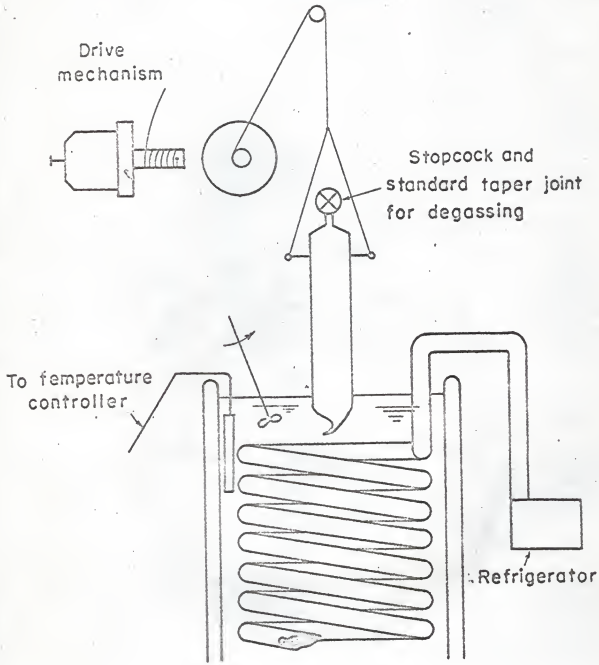

Fig. 5-1. Schematic diagram of the normal freezing apparatus.

Temperature profiles were determined in both the liquid and solid phases.

A tube specially designed to produce a monocrystal was used for the study of constitutional supercooling. This tube had a spiral capillary end as recommended by Spendiarov and Aleksandov (11) for growing single anthracene crystals. For all runs, it was necessary to remove dissolved gas from the specimen. This was accomplished by submerging the entire tube in the bath until the contents had become solid, then evacuating the tube and allowing the solid to melt. When this process was repeated three times, the specimen was effectively degassed, and no bubble formation during normal freezing was observed. To be certain the degassing process did not redistribute the solute, the liquid was mixed by rocking the tube in order to insure a uniform composition before each run.

B. Experimental Procedure

In making a typical experimental run, the tube with spiral capillary end was filled with approximately 40 grams of the specimen solution. After nucleating a small crystal with a cold source in the capillary spiral, the tube was hung vertically over and just touching the bath by rotating the shaft of the clockmotor. The motor was turned on and the tube allowed to descend into the bath. Usually, it would take several days for the completion of a run. After the entire specimen had frozen, the drive was stopped and the tube was raised incrementally, so that approximately one seventh of the specimen melted each time. Generally, two hours were required to complete the melting of each portion. Care was exercised at this point, as the interface tends to be rounded. However, upon standing a time, the interface becomes flat. Each melted portion was

transferred to a weighing bottle and weighed to 1/10 milligram.

A Baush and Lomb refractometer was used to measure the refractive index of each increment. A composition curve versus refractive index had been determined from mixtures of known composition and was used to convert refractive indices to compositions. All the refractive indices were read at 25.0°C to an accuracy of ± 0.0001. The calibration curves for all systems employed in this work are given in Appendices III, IV, and V.

C. Systems

For the purpose of experimental investigation of the phenomena of constitutional subcooling, only binary solutions of the eutectic-forming type were employed. The reason for this choice is due to the advantage that if one controlled the bath temperature considerably above the eutectic temperature, the presence of solute (impurity) can only be explained in terms of liquid trapping.

Three systems were investigated:

Cyclohexane solute in benzene solvent,

Benzene solute in cyclohexane solvent,

Chloroform solute in benzene solvent.

For all three systems, the initial concentrations were very low, (approximately 1 mole %), but the minimum workable concentration was restricted by the uncertainty in the composition analysis.

The benzene and cyclohexane used in this study were Phillips Petroleum Company's pure grade hydrocarbons. The chloroform was a Fisher Scientific Company's Certified Reagent. The solutes and solvents were subjected to no special treatment before use.

VI. EXPERIMENTAL RESULTS AND DISCUSSIONS FOR TEMPERATURE PROFILES AND CONSTITUTIONAL SUBCOOLING

A. Imposed Temperature Profiles

The imposed temperature profile plays an important role in the occurrence of constitutional subcooling, as may be seen from equations (4-11) and (4-12). The quasi-steady state treatment presented in Chapter IV yielded the following expression for the imposed temperature profile in normal freezing:

$$\frac{T - T_a}{T_e - T_a} = \exp\left(-\frac{R_z + \sqrt{R_z^2 + 4\alpha\beta}}{2\alpha} z\right) \qquad (4 - 4).$$

Equation (4-4) indicates that a plot of $\ln \frac{T - T_a}{T_e - T_a}$ versus z should give a straight line with slope equal to $-\frac{R_z + \sqrt{R_z^2 + 4\alpha\beta}}{2\alpha}$. The term T_a in equation (4-4) refers to ambient temperature and was assumed constant in the derivation. It is very close to the room temperature everywhere except the position near the surface of the freezing bath. This ambient temperature has been measured at various positions near the bath. The temperature readings are presented in Table 1.

TABLE I. AMBIENT TEMPERATURE NEAR THE BATH

Distance from freezing interface, inch	Temperature °C
0	7.0
1½	17.4
2½	21.0
∞	25.5

Based on this data, an average ambient air temperature for that section between 0 and 2 cm from the interface (the region in which the temperature measurements were made) would be 15 $\pm 2^{o}$C.

From the expression for the imposed temperature profile, the liquid temperature gradient at the freezing interface can be obtained by simply differentiating equation (4-4) with respect to z and letting z equal zero. Thus,

$$G = (T_a - T_o)\frac{R_z + \sqrt{R_z^2 + 4\alpha\beta}}{2\alpha} \qquad (6-1).$$

Temperature measurements have been made for several runs. The semi-log plots of experimental results using pure benzene under two different freezing rates are presented in Figure (6-1). Both of these runs give straight lines as predicted by equation (4-4).

A further test of equation (4-4) would be to calculate the heat transfer coefficients and determine if their values lie in a reasonable range. The value of heat transfer coefficients can be calculated from the slope of those semi-log plots along with known freezing rate, R_z, and thermal diffusivity, α.

The calculated values of heat transfer coefficients are presented in Table II, which shows that h for both runs is essentially constant, as one would expect, and is in good agreement with the range of 0.2 - 10 given by McAdams (15).

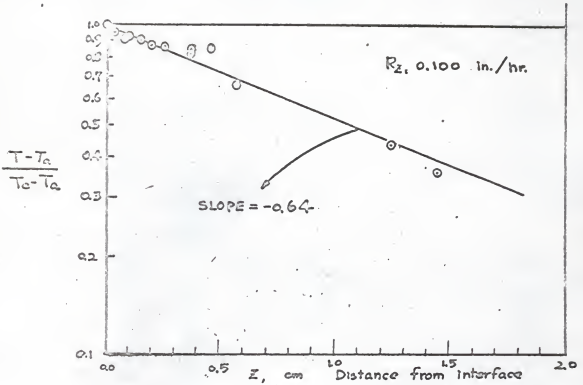

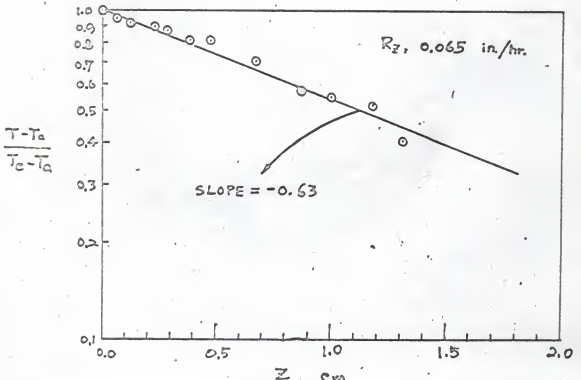

Fig. 6-1 Logarithm $\left(\frac{T-T_a}{T_e-T_a}\right)$ versus z for two different freezing rates.

TABLE II. VALUES OF HEAT TRANSFER COEFFICIENTS CALCULATED FROM EXPERIMENTAL DATA

RUN NO.	R_z (in - hr^{-1})	h(BTU hr^{-1} ft^{-2} $^oF^{-1}$)
II - 7	0.065	0.40
II - 8 & 9	0.100	0.41

Discussions

Effect of Natural Convection in the Liquid It is obvious that in the liquid phase, natural convection caused by temperature differences and/or density differences during normal freezing is possible. In problems such as this, the usual procedure is to employ an "effective thermal conductivity," k_{eff}; however, it is unnecessary in this problem. Equation (4-4) gives the shape of the temperature profile as exponential with distance from the interface, and it contains two adjustable constants, α and β.

Here, it was convenient to compensate for the neglect of natural convection effects in the liquid by adjusting the value of the heat transfer coefficient contained within β. The justification for this procedure is found in the good fit of the data to equation (4-4) and in the fact that the value of the heat transfer coefficient is quite reasonable.

Ambient Temperature, T_a As shown in Figure (6-1), the imposed temperature profile has the form of exponential decay with respect to distance from the interface, z, provided the ambient temperature is constant. However, the measured ambient temperature near the freezing interface is not constant but varies with z. It is obvious that T_a would be a function of z in equation (4-3); hence, instead of a constant

coefficient, a variable coefficient ordinary differential equation seems more reasonable. However, an averaged ambient temperature by direct measurement in the short range near the freezing interface satisfies the physical situation and conveniently simplifies the mathematical manipulations.

B. Constitutional Subcooling

In order to investigate the phenomenon of constitutional subcooling, a series of runs were performed with dilute solutions of eutectic-forming organic mixtures at very low freezing rates (0.065 to 0.1 inch per hour).

Three systems were investigated:

(1) Cyclohexane solute in benzene solvent,

(2) Benzene solute in cyclohexane solvent,

(3) Chloroform solute in benzene solvent.

The densities of each component at 20°C are (16):

Benzene	0.8790	g/ml
Cyclohexane	0.7791	g/ml
Chloroform	1.4984	g/ml

Solid-liquid equilibria have been reported for these two systems (16) and each has been found to exhibit simple eutectic behavior with no solid solution formation. The phase diagrams for these two systems are given in Appendices I and II.

As was mentioned in Chapter IV, two different models have been proposed to describe the occurrence of constitutional subcooling.

Boundary-Layer Model

The instability condition as expressed by the boundary layer

approach, equation (4-12), can be put in the following form:

$$\frac{1}{1 - g_p} = \frac{DG}{mR_z C_o} \exp\left\{-\frac{\delta R_z}{D}\right\} \qquad (6 - 2).$$

In order to test this relationship, the fraction of pure benzene obtained by normal freezing was experimentally determined for benzene-cyclohexane solutions of various initial concentrations at each of two freezing rates. These results are presented in Table III. If one takes logarithms and rearranges equation (6-2), the following expression is obtained:

$$\ln \frac{1}{1 - g_p} = \ln \frac{1}{C_o} + \ln \frac{DG}{mR_z} - \frac{\delta R_z}{D} \qquad (6 - 3).$$

For a given system at a constant freezing rate, equation (6-3) indicates that a plot of $\ln(\frac{1}{1 - g_p})$ versus $\ln(\frac{1}{C_o})$ should result in a straight line of unit slope. Figure (6-2) shows that the experimental results for each of the two freezing rates, given in Table III, are fitted quite well by straight lines with unit slope, as predicted.

TABLE III. FRACTION OF CHARGE OBTAINED AS PURE SOLVENT FOR VARIOUS INITIAL CONCENTRATIONS AT TWO DIFFERENT FREEZING RATES FOR CYCLOHEXANE IN BENZENE SYSTEM

Run No.	C_o (mole % benzene)	θ_p	R_z (inches per hour)
I-15	1.3	0.443	0.065
I-21	1.0	0.479	0.065
I-22	1.3	0.259	0.065
II-2	1.0	0.53	0.065
II-3	0.6	0.732	0.065
II-4	1.76	0.0835	0.065
II-6	0.35	0.818	0.065
I-16	0.45	0.587	0.100
I-18	0.81	0.265	0.100
I-19	0.48	0.478	0.100
I-20	0.25	0.729	0.100

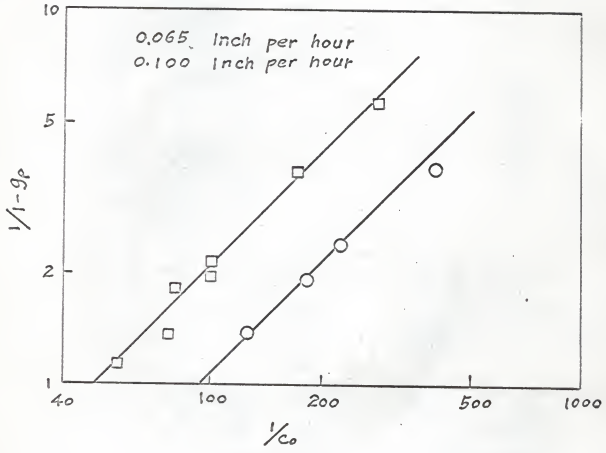

Fig. 6-2 Logarithm $(\frac{1}{1-g_p})$ versus logarithm $(\frac{1}{C_o})$ for cyclohexane solute in benzene solvent.

A further test of equation (6-2) would be to evaluate the boundary layer thickness, δ, and determine whether this parameter is realistic. One value of δ can be evaluated for each freezing rate, providing the temperature gradients at the interface, the diffusivity, and the slope of the liquidus line are known. The slope of the liquidus curve was calculated (17) with the assumption that the solution behaved ideally, and the diffusivity was estimated by the method of Wilke and Chang (18). These quantities are $66^{\circ}C$/mole fraction and $1.4 \times 10^{-5} cm^2/sec$, respectively. The temperature gradients for each freezing rate determined from Figure (6-1) are $6.3^{\circ}C$/cm and $6.4^{\circ}C$/cm for freezing rates of 0.065 in/hr and 0.100 in/hr, respectively.

Using those numerical quantities in equation (6-2), the calculated values of δ are 0.10 cm and 0.12 cm, respectively, for R_z = 0.065 in/hr and R_z = 0.100 in/hr. These caloulated values of δ are slightly larger than the range of 10^{-3} to 10^{-1} cm quoted by Chalmers (13), but are well within the range of 0.05 to 1.0 cm obtained by Wilcox (8) from an experimental study of zone melting of organic systems. They, thereby, add support to the boundary layer model.

The fact that the same value of δ was obtained for each freezing rate provides additional support. For it is expected that δ should be a function only of liquid phase agitation, and therefore, for freezing rates considerably lower than the convective flow, one would expect δ to be independent of freezing rate.

The fact that the calculated values of δ were found independent of freezing rate, and that heat transfer coefficients evaluated from the temperature profile data were also independent of freezing rate, suggests

a slightly different treatment of the data presented in Figure (6-2).

If the term G in equation (6-2) is eliminated by means of equation (6-1), the resulting equation, in effect, contains two parameters, namely, the boundary-layer thickness, δ, and the heat transfer coefficient which is included in β:

$$\frac{C_o}{1 - \epsilon_p} = \frac{D(T_a - T_e)}{2m\alpha} \left\{1 + \sqrt{1 + \frac{4\alpha\beta}{R_z^2}}\right\} \exp\left(-\frac{\delta R_z}{D}\right) \qquad (6 - 4).$$

Following the above discussion, these two parameters should be independent of freezing rate and could be evaluated from the two lines in Figure (6-2) by a trial-and-error procedure. The parameters so determined were δ = 0.11 cm and h = 0.42 BTU hr^{-1} ft^{-2} $^oF^{-1}$, which shows fairly good agreement with the values previously calculated. Thus, the same value of heat transfer coefficient has been determined from temperature profile measurements and mass transfer measurements.

Although constitutional subcooling in this system appears to be explained quite well in terms of the boundary-layer model, the experimental data were also compared against the diffusion model. This model, equation (4-14), however, predicts yields of pure benzene* much less than were observed. For example, a 0.4 mole % solution frozen at a rate of 0.10 inch per hour yielded 59% of the initial charge as pure benzene, while equation (4-10) predicts yields of 3% to 6% based on the experimentally determined range of the temperature gradient, G.

---

*It will be noted that the boundary layer model expresses the yield as a fraction frozen, while the diffusion model gives the time at which constitutional subcooling occurs. The fractional yield is easily calculated for the diffusion model using the freezing rate, tube diameter, and amount of charge by equation (3-11).

$$\tau = \frac{gL}{} \qquad (3 - 11)$$

From a fluid-mechanical viewpoint, the system under study can be described as a quiescent liquid above a horizontal solid surface enclosed within a relatively small diameter tube. Heat and mass transfer processes occur within the system and, therefore, temperature and concentration gradients exist in the liquid. Although the evidence in favor of the boundary-layer model is convincing, the success is, nevertheless, surprising, because this fluid-mechanical description of the system would seem to suggest the appropriateness of the diffusion model. The most obvious explanation is that some degree of liquid mixing exists as a result of free convection currents. Thermally induced free convection would appear to be absent because the temperature gradient is such that the lowest temperature occurs next to the interface. However, for this system, there is the possibility of free convection induced by concentration gradients. The concentration of cyclohexane is highest at the interface; and, because an increase in cyclohexane results in a decrease in liquid density, the liquid next to the interface would be less dense than the bulk liquid. This mechanism was also invoked by Wilcox (8) to explain results obtained from zone melting mixtures of organic compounds.

To test this free convection mechanism, attempts were made to obtain pure cyclohexane by normal freezing of dilute solutions of benzene in cyclohexane. Here, concentration induced density gradients should not lead to free convection, and one might expect this system to be described better by the diffusion model.

Diffusion Model

Both equations (4-11) and (4-12) contain the dimensionless group

$(\frac{DG}{mR_z C_o})$ which indicates the extent of constitutional subooooling. With the system of benzene solute in cyclohexane solvent, the value of the diffusivity will be the same as before; but m, the slope of the liquidus curve, was calculated to be 2.44°C/mole% (17) for cyclohexane as opposed to 0.66°C/mole% for benzene. The gradient, G, is expected to be the same order of magnitude. Hence, operating conditions for the production of pure cyclohexane should be more stringent (smaller R_z and C_o) than were necessary for the product of pure benzene. This was verified experimentally when it was observed that a 1 mole % solution of benzene in cyclohexane frozen at a rate of 0.065 inch per hour produced no pure cyclohexane; while at the same freezing rate, a one mole % solution of cyclohexane in benzene yielded approximately ±50% of the charge as pure benzene. Because of the uncertainty in analyzing the dilute solutions required for the production of pure cyclohexane, it was not possible to test equations (4-11) and (4-12) quantitatively with this system. However, several solid phase composition profiles were obtained at various freezing rates and initial concentrations. All profiles were similar to that shown in Figure (6-3) and exhibited the characteristic steady state region $(C/C_o = 1.0)$ required by the diffusion model.

This type of profile is similar to that expected for systems forming solid solutions. However, it has been shown that when trapping occurs, eutectic systems behave like solid solution systems. For when trapping occurs, the apparent solid phase concentration can be given by

$$C_s = fC_{z=0} \qquad (6-5)$$

where f is the surface void fraction. This expression may thus be regarded as a pseudo-distribution relationship which is analogous to that for a

solid solution. Where equation (6-5) is valid, one expects that solid phase profile equations derived for solid solutions would also apply to eutectic systems (17).

Referring to Figure (6-3), the area enclosed by $C/C_o = 1.0$ and the solid-phase concentration profiles from $g = 0$ to the steady state region is a measure of the segregation obtained by normal freezing. An analytical expression for this area can be obtained using the solid-phase profile equation derived by Tiller, et al., (2) for systems with nonzero distribution coefficients. Here, the distribution coefficient, K_o, has been replaced by the surface void fraction, f.

$$\int_0^{g_{ss}} \left(1 - \frac{C_s}{C_o}\right) dg = \frac{(1 - f)}{f \frac{Rl}{D}} \left\{1 - \exp\left(-f g_{ss} \frac{Rl}{D}\right)\right\} \qquad (6 - 6)$$

The left hand side of equation (6-6) is quite easily evaluated from the experimental solid-phase composition profile, and thus, a value of f may be calculated for each run. These calculated values of f are listed in Table IV, where it is observed that essentially the same value of f is obtained for each run. In terms of the trapping mechanism, this would imply that the interface morphology was essentially constant for all runs.

To further test the proposed composition induced free convection mechanism, chloroform solute in benzene solvent was investigated. This is another system in which concentration gradients produced by the freezing process should not induce free convection and, hence, should be described by the diffusion model.

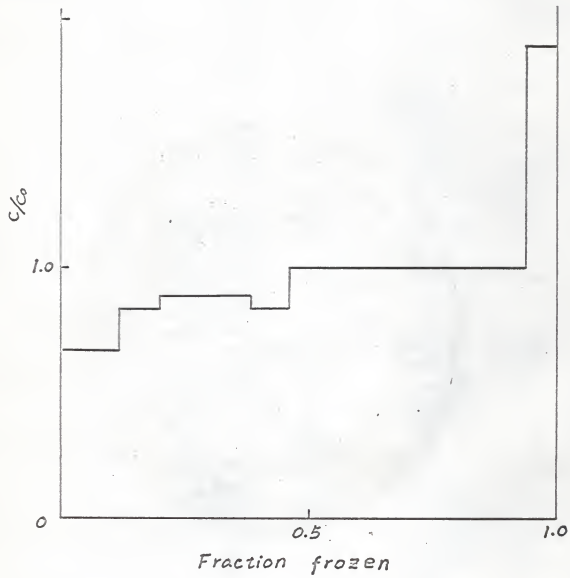

Fig. 6-3 A typical solid-phase composition profile for benzene solute in cyclohexane.

TABLE IV. VALUES OF f CALCULATED FROM EQUATION (6-6)

FOR BENZENE SOLUTE IN CYCLOHEXANE SOLVENT

RUN NO.	C_o (mole % benzene)	R_z (inches/hour)	f
II-11	1.00	0.065	0.085
II-12	1.85	0.130	0.080
III-1	2.00	0.100	0.080
III-2	2.00	0.100	0.085
III-3	2.00	0.163	0.085

When two dilute solutions were subjected to normal freezing at the lowest attainable freezing rate (0.065 inch per hour), the yields of pure benzene were found to be in agreement with the predictions of the diffusion model. A 0.42 mole % solution yielded 42% of the charge as pure benzene, while a 15% yield was obtained from a 0.55 mole % solution. Using the temperature gradients obtained from Figure (6-1), equation (4-11) predicts yields of 27 and 18% respectively, for these solutions.

While the adjustable parameter, δ, imparts considerable flexibility to the boundary layer model in correlating experimental results, it decreases the efficacy of the model for predictive purposes. Because yields predicted by this model depend rather strongly on the value of δ and tend to approach those of the diffusion model as δ becomes large, the problem lies in assigning a realistic value to this parameter. If the value obtained for the chloroform in benzene system (δ = 0.10 cm) is used along with the experimentally determined range of G, equation (4-12) predicts yields of 87% for the 0.42 mole % solution and 78% for the 0.55 mole % solution. Even if the boundary layer thickness is increased to 0.5 cm, the results (82% and 64%, respectively) are still much higher than found experimentally. It, therefore, seems safe to state that this system is described better by the diffusion model.

VII. CONCLUSION

It has been shown that the boundary layer model is applicable to normal freezing of the Benzene-Cyclohexane system, and that the diffusion model is applicable to the Cyclohexane-Benzene and Benzene-Chloroform systems. Because these two groups of systems can also be classified on the basis of the variation of liquid density with solute concentration, it is concluded that when the liquid density of the solute is less than that of the solvent, free convection will occur and the boundary layer model is appropriate. Conversely, when the liquid density of the solute exceeds that of the solvent, no free convection is possible and the diffusion model is appropriate.

With the appropriate model, the onset of constitutional subcooling can be correlated and reliably predicted by means of theoretical equations. Although equations have been applied only to normal freezing here, equations based on the same stability criterion can be derived easily for the related process of zone melting. The most striking manifestation of this phenomenon is the severity of operating conditions required to produce pure material from eutectic-forming organic systems.

Where conditions are such that constitutional subcooling exists, liquid is trapped by the resulting irregular interface as freezing occurs. The results from several systems show that under these conditions normal freezing of eutectic systems produces solid phase composition profiles characteristic of systems forming solid solutions. The effective distribution coefficient for such systems can be explained in terms of a surface void fraction.

ACKNOWLEDGMENT

The author wishes to express his sincere appreciation to Dr. Benjamin G. Kyle, whose advice and consultation have contributed very greatly to the completion of this work. I also wish to express my thanks to the Computer Center of Kansas State University for the use of IBM 1410 Computer.

APPENDIX I. PHASE DIAGRAM FOR BENZENE—CYCLOHEXANE SYSTEM.

(Timmermans, "Physico-Chemical constants of Binary Systems," vol. 3, Interscience (1960).)

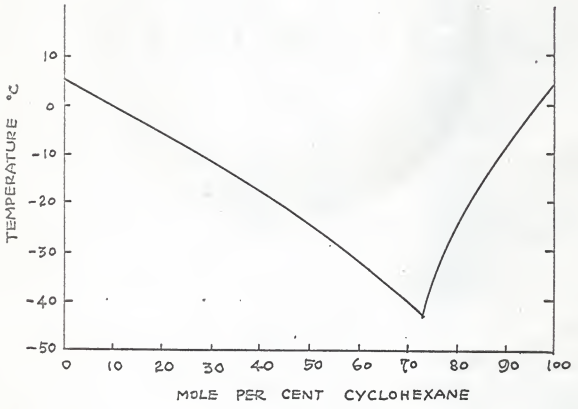

APPENDIX II. PHASE DIAGRAM FOR BENZENE-CHLOROFORM SYSTEM

(Timmermans, "Physico-Chemical constants of Binary Systems," vol. 3, Interscience (1960))

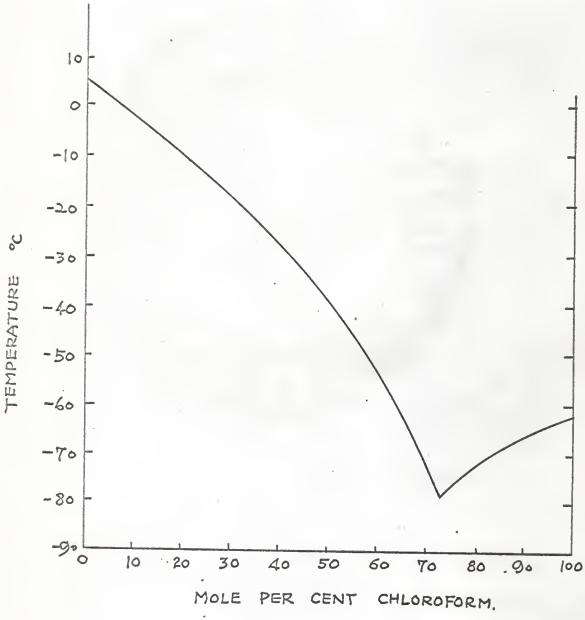

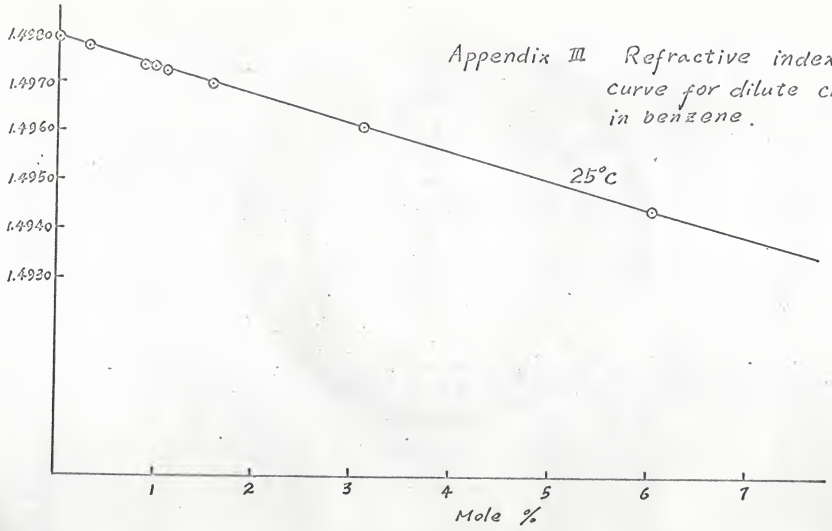

Appendix III Refractive index curve for dilute chloroform in benzene.

Appendix IV Refractive index curve for dilute cyclohexane in benzene.

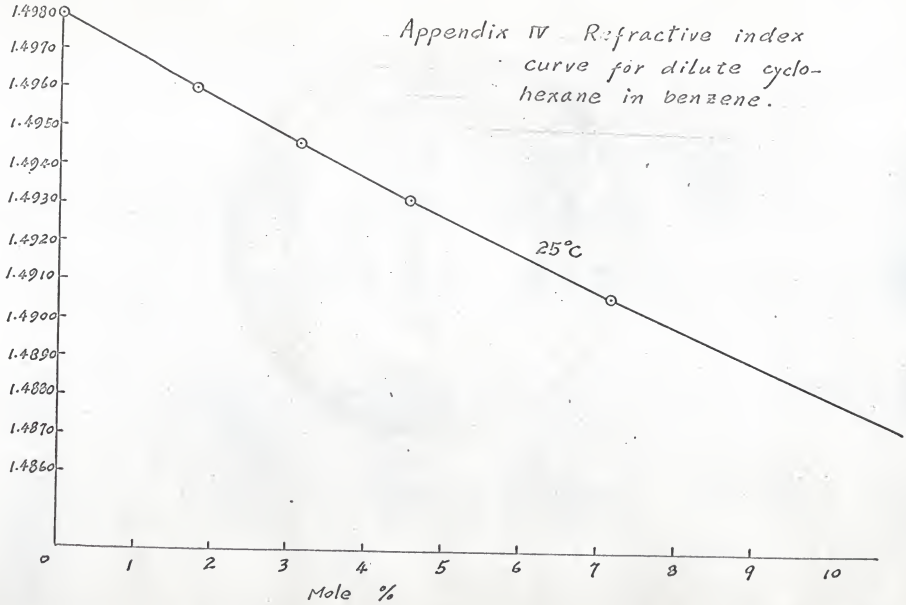

Appendix V Refractive index curve for dilute benzene in cyclohexane.

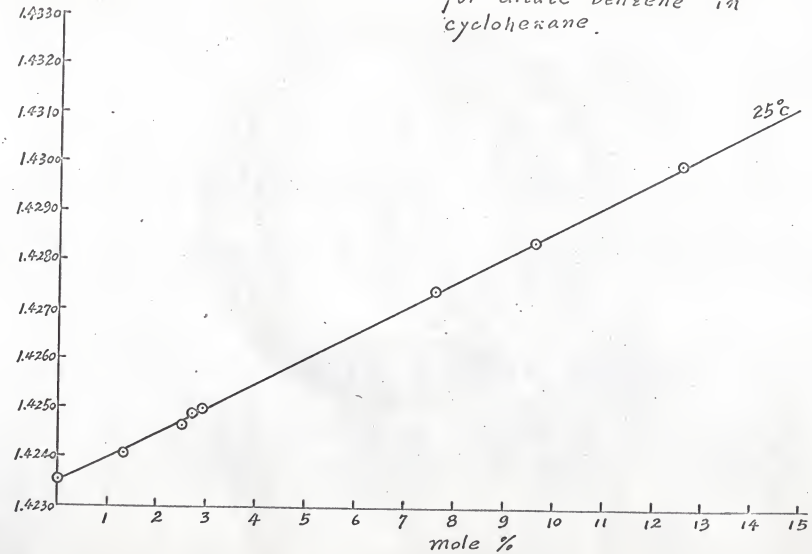

APPENDIX VI. TYPICAL COMPUTER PROGRAM

FOR FINITE-DIFFERENCE CALCULATIONS

```
      DIMENSIONC(50),CL(50)
100   FORMAT(5H RLD=F10.2)
101   FORMAT(3H P=F6.4)
102   FORMAT(6F12.6)
200   FORMAT(6H TIME=F10.2)
201   FORMAT(10F12.6)
202   FORMAT(F12.6)
      DX=0.05
      DT=0.00125                                  PARAMETERS
      RLD=10. - - - - - - - - - - 1/δ
      B=1     - - - - - - - - - - b
      P=0.02  - - - - - - - - - - K_o
      WRITE(3,101)RLD
      READ(1,202)(C(J),J=1,22)
      L=1
      K=1
      CO=((1.+(1.-P)*DX)/(1.-(1.-P)*DX))*C(3)
      C(1)=(CO+C(1))/2.
    1 DO2J=2,21
      AK=K+100*(L-1)
    2 CL(J)=(0.5+DT/(DX*2.))*C(J+1)+(0.5-DT/(DX*2.))*C(J-1)
      CL(1)=((1.+(1.-P)*DX)/(1.-(1.-P)*DX))*CL(3)
      CL(22)=(C(21)-C(22))*(1./(B*(DX/DT)*(RLD-1.)-AK*DX))+C(22)
      IF(K-100)3,3,4
    3 DO 5 J=1,22
    5 C(J)=CL(J)
      K=K+1
      GO TO 1
    4 CS=P*CL(2)
      WRITE(3,200)AK
      WRITE(3,201)(CL(J),J=2,22)
      WRITE(3,202)CS
      L=L+1
      K=K-100
      C(J)=CL(J)
      K=K+1
      GO TO 1
      END
1.0          1.0          1.0          1.0          1.0          1.0
1.0          1.0          1.0          1.0          1.0          1.0
1.0          1.0          1.0          1.0          1.0          1.0
1.0          1.0          1.0          1.0
```

NOMENCLATURE

a, a_1, a_2 — constants of integration

A — cross-sectional area of glass tube, cm^2

$b = \delta R_z/D$ — dimensionless boundary layer thickness

C — solute concentration in liquid at distance z from interface, mole-fraction

C_b — bulk liquid concentration, mole-fraction

C_e — eutectic composition, mole-fraction

C_o — initial solute concentration in liquid, mole-fraction

C_p — heat capacity, $cal/gm\,^oC$

C_s — solute concentration in solid, mole-fraction

D — binary diffusivity, cm^2/sec

$G = \left(\frac{dT}{dz}\right)_{z=0}$ — temperature gradient in liquid phase at the freezing interface, $^oC/cm$

g — fraction frozen

g_o — fraction frozen for initial period

g_p — fraction of charge obtained as pure solvent

g_{ps} — fraction of charge obtained at the onset of subcooling (solid solution system)

g_{ss} — fraction frozen when steady state is reached (diffusion model)

h — heat transfer coefficient between the tube and the ambient air

K_o — equilibrium distribution coefficient

K_E — effective distribution coefficient

k — thermal conductivity

l — the length of total charge, cm

$L = \frac{lR_z}{D}$ — the length of total charge, cm

m — slope of liquidus line

R_z — rate of freezing

R — radius of tube

t — time

T — temperature in the liquid

T_a — temperature of surroundings

T_e — equilibrium temperature of the solution in contact with the interface

T_E — equilibrium temperature

T_o — freezing point of the solvent

Z_o — distance down solid from first solid frozen out

z — distance from interface

Z — incubation distance for diffusion model

α — thermal diffusivity

$\beta = \frac{2h}{R_z \rho_l C_p}$ — dimensionless heat transfer group

δ — boundary-layer thickness, cm

$\xi = \frac{C_e}{C_o}$ — relative eutectic composition

$\eta = \frac{zR_z}{D}\left(\frac{\rho_s}{\rho_l}\right)$ — dimensionless distance from interface

ρ_s — density of solid

ρ_l — density of liquid

$\tau = \frac{tR_z^2}{D}\left(\frac{\rho_s}{\rho_l}\right)^2$ — dimensionless time

τ_o — duration of initial period

τ_t — dimensionless time from beginning of terminal period, $\tau_t = (\tau - \tau_o)$

$\phi = C/C_o$ — dimensionless concentration

$\phi_b = C_b/C_o$ — dimensionless bulk concentration

$\phi_s = C_s/C_o$ — dimensionless solute concentration in solid

BIBLIOGRAPHY

1. Pfann, W.G., J. Metals, 4, 747 (1952).

2. Tiller, W.A., Jackson, K.A., Rutter, J.W., and Chalmers, B., Acta Met., 1, 428 (1953).

3. Smith, V.G., Tiller, W.A., and Rutter, J.W., Can. J. Phys., 33, 723 (1955).

4. Hulme, K.F., Proc. Phys. Soc., B68, 393 (1955).

5. Wilcox, W.R., J. Appl. Phys., 35, 636 (1964).

6. Wagner, C., Trans AIME, 200, 154 (1954).

7. Burton, J.A., Prim, R.C., and Slichter, W.P., J. Chem. Phys., 21, 1987 (1953).

8. Wilcox, W.R., Ph.D. Thesis, University of California, Berkeley, Cal., 1960.

9. Rutter, J.W., and Chalmers, B., Can. J. Phys., 31, 15 (1953).

10. Pfann, W.G., "Zone Melting," John Wiley and Sons, New York, 1958.

11. Spondiarov, N.N., and Aleksandov, B.S., "Growth of Crystals," vol. 2, p.61, Consultant Bureau, Inc., New York, 1959.

12. Wilcox, W.R., Air Force Report No. AF 04(695)-165, 1963.

13. Chalmers, B., "Principles of Solidification," p. 142. John Wiley and Sons, New York, 1964.

14. Landau, A.I., in Rost Kristallov, First Conference on Crystal Growth (Academy of Sciences USSR Press, Moscow, 1957), p.58.

15. McAdams, W.H., "Heat Transmission," 3rd ed., p. 5, McGraw-Hill Book Company, Inc., New York, 1954.

16. Timmermans, J., "Physico-Chemical Constants of Binary Systems," Vol. 3, Interscience, New York, 1960.

17. Private communication with B.G. Kyle.

18. Wilke, C.R., and Chang, P., A.I.Ch.E.J., 1, 270 (1955).

19. Landau, A.I., POMM, 6, 132 (1958).

TRANSPORT PROCESSES ACCOMPANYING FREEZING

by

CHON SHON CHENG

B.S., National Taiwan University, 1964

AN ABSTRACT OF A MASTER'S THESIS

submitted in partial fulfillment of the

requirements for the degree

MASTER OF SCIENCE

Department of Chemical Engineering

KANSAS STATE UNIVERSITY

Manhattan, Kansas

1967

Normal freezing of three eutectic-forming organic systems has been studied experimentally and the occurrence of constitutional subcooling has been clearly established. This phenomena, previously observed in systems of metallurigical interest and until now only postulated in organic systems, results in the instability of a planar solid/liquid interface and leads to solute trapping. This trapping mechanism quantitatively explains why eutectic-forming systems exhibit solid-phase concentration profiles identical to those expected of systems which form solid solutions. The onset of constitutional subcooling can be correlated and reliably predicted by means of theoretical equations.

In order to derive the expressions for the onset of constitutional subcooling, the temperature profile in the liquid phase has been set up based on a simplified model. It is shown to be in fairly good agreement with directly measured temperature data.

The approximation of quasi-steady state employed in solving the concentration profile of the boundary-layer model has been discussed and compared with an exact solution obtained from a finite-difference calculation.

Although the process of normal freezing with no liquid phase agitation would appear well-described by a diffusion model, free convection induced by concentration gradients renders a boundary layer more appropriate when the liquid density of the solvent exceeds that of the solute.